Paleoceanography and Paleoclimatology

RESEARCH ARTICLE
10.1029/2020PA003962

Coral Record of Younger Dryas Chronozone Warmth on the Great Barrier Reef

Logan D. Brenner[1], Braddock K. Linsley[2], Jody M. Webster[3], Donald Potts[4], Thomas Felis[5], Michael K. Gagan[6,7], Mayuri Inoue[8], Helen McGregor[6], Atsushi Suzuki[9], Alexander Tudhope[10], Tezer Esat[11], Alex Thomas[10], William Thompson[12], Stewart Fallon[11], Marc Humblet[13], Manish Tiwari[14], and Yusuke Yokoyama[15]

[1]Department of Environmental Science, Barnard College, New York, NY, USA, [2]Lamont-Doherty Earth Observatory, Palisades, NY, USA, [3]Geocoastal Research Group, School of Geosciences, The University of Sydney, Sydney, New South Wales, Australia, [4]Department of Ecology and Evolutionary Biology, University of California, Santa Cruz, Santa Cruz, CA, USA, [5]MARUM—Center for Marine Environmental Sciences, University of Bremen, Bremen, Germany, [6]School of Earth, Atmospheric and Life Sciences, University of Wollongong, Wollongong, New South Wales, Australia, [7]School of Earth and Environmental Sciences, The University of Queensland, St Lucia, Queensland, Australia, [8]Department of Earth Sciences, Okayama University, Tsushima-naka, Japan, [9]Geological Survey of Japan, National Institute of Advanced Industrial Science and Technology, Tsukuba, Japan, [10]School of GeoSciences, University of Edinburgh, Edinburgh, UK, [11]Research School of Earth Sciences, The Australian National University, Canberra, ACT, Australia, [12]Department of Geology and Geophysics, Woods Hole Oceanographic Institution, Woods Hole, MA, USA, [13]Department of Earth and Planetary Sciences, Nagoya University, Nagoya, Japan, [14]National Centre for Polar and Ocean Research, Ministry of Earth Sciences, Vasco-da-Gama, India, [15]Atmosphere and Ocean Research Institute, The University of Tokyo, Kashiwa, Japan

Key Points:
- Near-modern sea surface temperatures were reached during the Younger Dryas Chronozone on the Great Barrier Reef
- Sea surface temperature, reef assemblage, and sea level data provide an overview of the evolution of the Great Barrier Reef since the LGM
- *Isopora*-based sea surface temperature calibrations can be applied to fossil *Isopora* to understand environmental change on coral reefs

Supporting Information:
- Supporting Information S1

Correspondence to:
L. D. Brenner,
lbrenner@barnard.edu

Citation:
Brenner, L. D., Linsley, B. K., Webster, J. M., Potts, D., Felis, T., Gagan, M. K., et al. (2020). Coral record of Younger Dryas Chronozone warmth on the Great Barrier Reef. *Paleoceanography and Paleoclimatology*, *35*, e2020PA003962. https://doi.org/10.1029/2020PA003962

Received 20 APR 2020
Accepted 1 DEC 2020
Accepted article online 11 DEC 2020

Abstract The Great Barrier Reef (GBR) is an internationally recognized and widely studied ecosystem, yet little is known about its sea surface temperature (SST) evolution since the Last Glacial Maximum (LGM) (~20 kyr BP). Here, we present the first paleo-application of *Isopora* coral-derived SST calibrations to a suite of 25 previously published fossil *Isopora* from the central GBR spanning ~25–11 kyr BP. The resultant multicoral Sr/Ca- and $\delta^{18}O$-derived SST anomaly (SSTA) histories are placed within the context of published relative sea level, reef sequence, and coralgal reef assemblage evolution. Our new calculations indicate SSTs were cooler on average by ~5–5.5°C at Noggin Pass (~17°S) and ~7–8°C at Hydrographer's Passage (~20°S) (Sr/Ca-derived) during the LGM, in line with previous estimates (Felis et al., 2014, https://doi.org/10.1038/ncomms5102). We focus on contextualizing the Younger Dryas Chronozone (YDC, ~12.9–11.7 kyr BP), whose Southern Hemisphere expression, in particular in Australia, is elusive and poorly constrained. Our record does not indicate cooling during the YDC with near-modern temperatures reached during this interval on the GBR, supporting an asymmetric hemispheric presentation of this climate event. Building on a previous study (Felis et al., 2014, https://doi.org10.1038/ncomms5102), these fossil *Isopora* SSTA data from the GBR provide new insights into the deglacial reef response, with near-modern warming during the YDC, since the LGM.

1. Introduction

The tropical Pacific's response to the deglaciation following the Last Glacial Maximum (LGM) remains poorly documented. The LGM is considered to be the coldest period in Earth's recent geologic history (e.g., Mix et al., 2001), and yet coral reefs persisted at this time (Montaggioni, 2005). The Great Barrier Reef (GBR), the largest (~344,400 km^2) extant epicontinental coral reef system (Davies et al., 1989), is situated on the southern edge of the Western Pacific Warm Pool (WPWP) and extends from ~10° to 22°S and from ~144° to 152°E (Figure 1). The initiation of the GBR is poorly constrained and controversial, occurring sometime between Martine Isotope Stages (MIS) 11 and 15 (see Humblet & Webster, 2017, for a recent summary), while exhibiting various morphologies and surviving both glacial and interglacial climates. Tracking sea surface temperature anomalies (SSTAs) on coral reefs over time could supplement molecular biogeographic studies (e.g., Palumbi, 1997) or those examining a potential genetic fingerprint in species who continue to thrive through glacial–interglacial transitions (e.g., Hewitt, 2000). To better understand the development of the GBR since the LGM, a suite of studies used Integrated Ocean Drilling Program Expedition 325 Great Barrier Reef Environmental Changes (IODP Expedition 325) fossil-reef core samples to evaluate changes

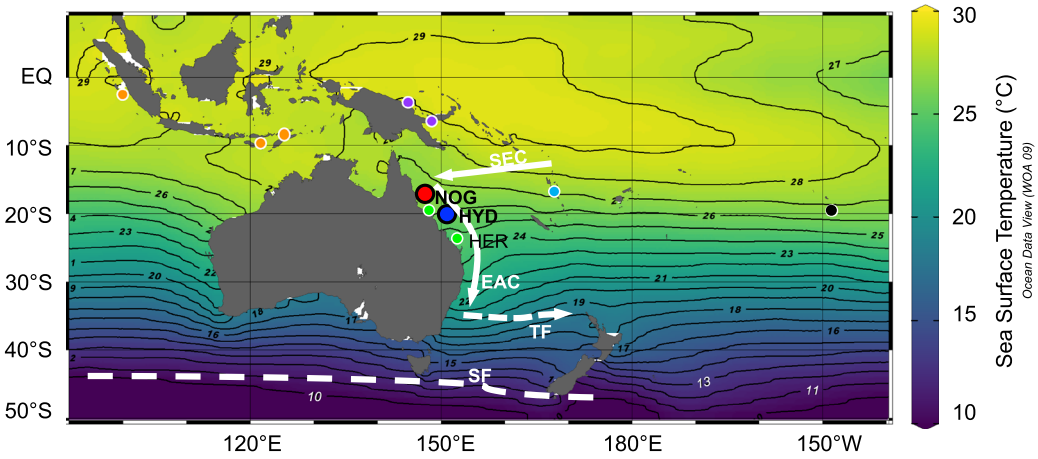

Figure 1. Map of study sites, Noggin Pass (17°S, NOG) and Hydrographer's Passage (20°S, HYD) in the GBR off the northeast coast of Australia in the Coral Sea with mean annual SST contours (reference period: 1955–2006, World Ocean Atlas 2009; Locarnini et al., 2010). The approximate locations of relevant major currents in the region, the South Equatorial Current (SEC), East Australian Current (EAC), and Tasman Front (TF) are denoted by arrows pointing in the direction of flow. The Subtropical Front (SF) is a surface water mass boundary. Heron Island Reef (HER), the site of the modern corals included in the Brenner et al. (2017) calibration is noted. The smaller colored markers represent the locations of Younger Dryas Chronozone and early Holocene fossil corals from other studies that will be utilized to contextualize warming on the GBR (orange: Indonesia, Abram et al., 2009; Gagan et al., 2004; green: GBR, Gagan et al., 2004; Sadler et al., 2016; purple: Papua New Guinea, Abram et al., 2009; Gagan et al., 2004; light blue: Vanuatu, Duprey et al., 2012; Gagan et al., 2004; black: Tahiti, Asami et al., 2009; Cohen & Hart, 2004; DeLong et al., 2010; Felis et al., 2012).

in sea level (Yokoyama et al., 2018), reef growth, structure, and coralgal assemblages (i.e., intergrowth of framework-building corals, algae, associated microbialite, and vertical accretion rates) (Humblet et al., 2019; Szilagyi et al., 2020; Webster et al., 2018), a meridional thermal gradient (Felis et al., 2014), regional sedimentation (Hinestrosa et al., 2019) and bioerosion (Patterson et al., 2020).

The first *Isopora*-based sea surface temperature (SST) calibrations were published by Felis et al. (2014) based on bulk-sampled modern *Isopora* from throughout the WPWP. However, in lieu of another *Isopora* calibration to serve as a comparison, a suite of previously published *Porites*-based SST calibrations (DeLong et al., 2010; Felis et al., 2009; Gagan et al., 2012) were applied to the IODP Expedition 325 corals. This revealed a larger meridional thermal gradient across the GBR during the last deglaciation (Felis et al., 2014). In this contribution, we revisit the IODP Expedition 325 corals to provide the first paleo-application of two *Isopora*-based SST calibrations with site-specific modern benchmarks to show uninterrupted warming since the LGM. In addition to the bulk-sampled calibration, we also apply an SST regression based on five, high-resolution (1-mm interval) sampled, modern *Isopora* from Heron Island south of our study sites, Noggin Pass (NOG, ~17°S) and Hydrographer's Passage (HYD, ~20°S) (Brenner et al., 2017) (Figure 1).

We elaborate on the earlier findings of relative sea surface ocean warmth on the GBR during the Younger Dryas Chronozone (YDC) (Felis et al., 2014), when at the same time the Northern Hemisphere was cooling. We also explore potential mechanisms for the poorly constrained Southern Hemisphere warmth and examine the GBR in the context of 52 coral Sr/Ca-derived SSTAs in the WPWP (Abram et al., 2009; Asami et al., 2009; Cohen & Hart, 2004; Corrège et al., 2004; DeLong et al., 2010; Duprey et al., 2012; Felis et al., 2012; Gagan et al., 2004; Sadler et al., 2016).

By incorporating a synthesis of the five-reef sequences that characterizes the GBR evolution since the LGM (Humblet et al., 2019; Webster et al., 2018; Yokoyama et al., 2018) we further contextualize our SSTA record. This allows us to explore how changing SSTs may have impacted or interacted with other environmental variables to influence the development of the GBR since the LGM. Each of these reefs is associated with unique changes in relative sea level (RSL) as well as coralgal assemblage shifts (Humblet et al., 2019; Webster et al., 2018; Yokoyama et al., 2018), discussed in detail in section 6.2, and considering the

corresponding SSTAs provide a thorough understanding of the GBR. However, important questions remain regarding the relative importance of sedimentation, temperature rise, and rising sea level in controlling reef demise.

2. Existing Thermal History of the Great Barrier Reef Since the LGM

Today, the relatively elevated SSTs on the GBR are largely maintained by surface ocean currents, namely the South Equatorial Current (SEC) and the East Australian Current (EAC). The SEC flows from the east to intersect with northeastern Australia. At this juncture, surface water flows southward as the EAC, which carries heat to the subtropical regions in the far western South Pacific. NOG and HYD are in the modern-day path of the EAC and the present-day average annual SSTs are 26.6°C and 26°C, respectively (World Ocean Atlas 2009 long-term climatological mean [reference period: 1955–2006]; Locarnini et al., 2010) (Figure 1).

Felis et al. (2014) measured Sr/Ca in *Isopora* corals collected on IODP Expedition 325 to provide the first tropical Pacific coral-based SST estimates for the LGM and showed that NOG and HYD were 4–6°C and 6–8°C cooler than present, respectively. From ~20 to ~13 kyr BP there was a meridional SST gradient of 2–3°C between NOG and HYD, much steeper than the ~0.6°C that spans the 3° of latitude separating these sites today (Felis et al., 2014). The steeper gradient was attributed to a weaker EAC, which allowed cooler and more saline southern subtropical waters to travel northward (Felis et al., 2014). By 12.7 kyr BP, the gradient weakened when HYD warmed more than NOG probably due to intensification of the South Pacific Subtropical Gyre and EAC (Bostock et al., 2006; Felis et al., 2014). This was possibly associated with a simultaneous southward shift in the southern edge of the WPWP and the Intertropical Convergence Zone (ITCZ) (Felis et al., 2014).

Coral $\delta^{18}O$ data from the same samples were corrected for glacial-interglacial ice volume changes and yielded a cooling of ~7°C (NOG) to 9°C (HYD) during the LGM compared to present (Felis et al., 2014). These temperature estimates are cooler than those derived from the Sr/Ca because changes in the regional $\delta^{18}O$ composition of seawater resulted in a positive anomaly of 0.4–0.8‰ in coral $\delta^{18}O$ (Felis et al., 2014). The source of this anomaly was also attributed to the weaker EAC. The subtropical water, more enriched in ^{18}O than the WPWP-sourced EAC, penetrated reefs to 20–17°S during the LGM and the following deglaciation (Felis et al., 2014). This was further than the ~25°S boundary previously identified by planktonic foraminiferal assemblages during the LGM (Anderson et al., 1989) and $\delta^{18}O$ during deglaciation (Bostock et al., 2006; Felis et al., 2014).

3. Younger Dryas Chronozone in the Southwestern Tropical Pacific Ocean

To date, there is no clear Australian climate expression for the YDC (12,850–11,650 calendar years before 1950; Rasmussen et al., 2006), which was originally defined as a sudden period of intense cooling in Europe with a correlative decrease in temperature in North America, the North Atlantic and North Pacific, and Asia (Clark et al., 2002; Shakun & Carlson, 2010). In Australia and the surrounding waters, there is some evidence for cooling (e.g., Andres et al., 2003) but a thorough review by Tibby (2012) concluded that there was no coherent SST pattern throughout southern and eastern Australia. Two additional reviews (Reeves, Barrows, et al., 2013; Reeves, Bostock, et al., 2013) suggest either no expression or subtle warming that was recorded by planktonic foraminifera south of Australia (De Deckker et al., 2012). With their original SSTA record, Felis et al. (2014) noted relative warming during the YDC in the central GBR, which diverged from other coral-based studies in Vanuatu (Corrège et al., 2004) and Tahiti (Asami et al., 2009) located at the same latitude as the GBR but ~2,000 km to the east in the South Pacific Ocean.

Multiple proxy studies using speleothems (e.g., Williams et al., 2004), pollen (e.g., Vandergoes et al., 2005), and foraminifera (e.g., Barrows et al., 2007) from nearby New Zealand support warming during the YDC; however, the majority of evidence for warming is from exposure dating of glacial moraines. Notably, Barrows et al. (2007) combined their foraminifera $\delta^{18}O$-based SST record from the neighboring Tasman Sea and pollen data (Vandergoes et al., 2005) with new and revised exposure ages of the Franz Josef Glacier on the South Island to overturn the prior notion of glacial advancement during the YDC. Since then, studies of New Zealand glaciers are consistently yielding evidence of warming during the YDC

(e.g., Kaplan et al., 2013; Kelley et al., 2014; Koffman et al., 2017; Putnam et al., 2010; Putnam, Schaefer, Denton, Barrell, Andersen, et al., 2013; Putnam, Schaefer, Denton, Barrell, Birkel, et al., 2013; Shulmeister et al., 2019; Strand et al., 2019). Although nearby, there are fewer proxy studies associated with this interval in Australia or on the GBR.

4. Methods

4.1. Coral Collection, Diagenesis Screening, and Geochemical Analysis

IODP Expedition 325 drilled through the seaward margins of drowned GBR reefs to collect fossil coral and coralline algal samples in February–April 2010. Samples were collected at NOG (17.1°S, 146.6°E) and HYD (19.7°S, 150.3°E) (Webster et al., 2011). For a complete map of drill sites refer to Yokoyama et al. (2018) and the IODP Expedition 325 proceedings (Webster et al., 2011). All samples are from drill cores that retrieved massive and robust branching/columnar fossil *Isopora palifera/cuneata* between 56 and 126 m below modern sea level and were described and prepared for sampling in Bremen, Germany in July 2010.

The geochemical data utilized in this paper were originally published in Felis et al. (2014) and the following summarizes the previously applied methods. The fossil corals were U-Th dated at three laboratories: Woods Hole Oceanographic Institution (WHOI), Australian National University (ANU), and University of Oxford (UO). Ages are reported in kyr BP and interlaboratory replication is within 100 years, approaching the intra-coral variation elucidated by high-precision methods at WHOI. For full U-Th and radiocarbon dating results, as well as the unique dating methods at each laboratory, see Yokoyama et al. (2018).

In order for a coral to be included in the SSTA record it must pass a tripartite screening for diagenesis: (1) Fossil corals were analyzed via powder X-ray diffraction and X-radiograph and must have ≤1.5% calcite and no obvious alteration, (2) petrographic thin sections did not indicate any significant amount of secondary aragonite or calcite with primary porosity preserved, and (3) Mg/Ca values were not indicative of high-Mg calcite and secondary aragonite (Felis et al., 2014). Sample-specific results of the screening can be found in Felis et al. (2014).

Sr/Ca and $\delta^{18}O$ analyses of fossil coral colonies (NOG: $n = 12$, HYD: $n = 13$) were conducted at MARUM-Center for Marine Environmental Sciences (Bremen, Germany), Lamont-Doherty Earth Observatory (Palisades, NY), ANU (Canberra, Australia), School of GeoSciences (Edinburgh, Scotland), The National Institute of Advanced Industrial Science and Technology (Tsukuba, Japan), and The Atmosphere and Ocean Research Institute (Kashiwa, Japan). Coral Sr/Ca was measured via inductively coupled plasma-optical emission spectrophotometry and -mass spectrometry and stable isotope analyses were conducted via dual-inlet stable-isotope ratio mass spectrometry. The coral reference material JCp-1 (Hathorne et al., 2013) was used to account for any interlaboratory offsets, and the JCp-1 reference compositions reported in Felis et al. (2014) are 8.781 mmol mol^{-1} for Sr/Ca and −4.75‰ for $\delta^{18}O$. The coral $\delta^{18}O$ values were adjusted using the Waelbroeck et al. (2002) glacial-interglacial $\delta^{18}O$ seawater composition record. Each reported coral Sr/Ca or $\delta^{18}O$ value is an average of at least triplicate analysis of bulk powder, or of an analysis of subseasonally microsampled powders ($n = 29$ to 232), to provide one average value representing an individual coral. See Felis et al. (2014) for further details on the geochemical analysis.

The reef sequences described in section 6.1 were distinguished based on lithologic, chronostratigraphic, and biologic criteria (Webster et al., 2018). The RSL envelopes for NOG and HYD were constructed based on U-Th coral ages and ^{14}C AMS (radiocarbon) coral and coralline algal ages with paleo-water depth established via a multiproxy approach including corals, coralline algae, algal crust thickness, and vermetid gastropod presence (Humblet et al., 2019; Webster et al., 2018; Yokoyama et al., 2018).

4.2. *Isopora* Calibration Application

All Sr/Ca and $\delta^{18}O$ values were corrected using JCp-1 to account for interlaboratory offsets and address analytical uncertainty prior to applying SST calibrations. Two sets of *Isopora*-based reduced major axis (RMA) SST-calibrations from Brenner et al. (2017),

$$\frac{Sr}{Ca} \times 10^3 = 11.37(\pm 0.02) - 0.083(\pm 0.007) \times SST,$$

$$\delta^{18}O = 0.65(\pm 0.04) - 0.185(\pm 0.014) \times SST,$$

and Felis et al. (2014),

$$\frac{Sr}{Ca} \times 10^3 = 11.15(\pm 0.09) - 0.075(\pm 0.011) \times SST,$$

$$\delta^{18}O = 1.6(\pm 0.5) - 0.218(\pm 0.027) \times SST,$$

were applied to the fossil coral measurements. The RMA treatment permits symmetrical use of the regressions (Smith, 2009) and is appropriate for calibration application. The Brenner et al. (2017) calibrations utilize five *Isopora* corals collected at Heron Island (151.9°E, 23.4°S) on the GBR, south of NOG and HYD (Figure 1). Each coral was drilled at 0.5-mm intervals, yielding 696 discrete samples, but values were averaged to 1-mm resolution after analysis and spanned 1971–1976 CE ($n = 3$) and 2009–2012 CE ($n = 2$). The Felis et al. (2014) calibration is based on 13 bulk sampled *Isopora*, collected 1974–1994, from off of Madang (145.8°E, 5.2°S) on the north coast of Papua New Guinea and three sites on the GBR, Myrmidon (147.4°E, 18.3°S), Magnetic Island (146.8°E. 19.1°S), and Heron Island.

With the absence of modern corals from NOG and HYD, we calculated a fossil-derived SST using one of the modern calibrations for Sr/Ca ($\delta^{18}O$) and subtracted this value from the corresponding modern benchmark (26.6°C [NOG] or 26°C [HYD] based on the World Ocean Atlas 2009 long-term climatological mean [reference period: 1955–2006] [Locarnini et al., 2010]) to yield an SSTA. We repeated the process for the other Sr/Ca ($\delta^{18}O$) regression, for a total of two sets of calibrations applied per coral. With site-specific benchmarks, these temperature estimates reflect local conditions.

The coral Sr/Ca data were also used to isolate the $\delta^{18}O$ of seawater ($\delta^{18}O_{sw}$) by removing the temperature signal from the total coral $\delta^{18}O$ value, similar to Gagan et al. (1998). For each coral we converted the Sr/Ca-derived SST from a given calibration into ‰ units with the matching $\delta^{18}O$-SST calibration. This temperature component is subtracted from the ice volume-corrected $\delta^{18}O$ value and the remainder is attributed to changes in the $\delta^{18}O_{sw}$. The process is repeated for the other set of *Isopora* calibrations, and both results are averaged together to produce one $\delta^{18}O_{sw}$ value per coral.

We calculated propagated uncertainty to accompany each SSTA value (Figures 2 and 3). The uncertainty calculation includes a first-order Taylor Expansion, following the methodology outlined by Bevington and Robinson (2002) and utilized in Brenner et al. (2017). The Taylor Expansion incorporates the standard error of the triplicate (at least) coral analyses and uncertainty associated with the calibration. Since the SST calibrations applied in this study were developed using multiple corals, they inherently capture the variability that is associated with a potential geochemical offset between coeval colocated corals. In addition to the Taylor expansion, we also consider the standard error of the mean modern SST benchmark (±0.19° for NOG and ±0.10°C for HYD). In the case of $\delta^{18}O_{sw}$, the uncertainty associated with the Sr/Ca-derived SST and the $\delta^{18}O$-SST calibration is considered. See supporting information for the complete error propagation equations. We applied weighted least squares (WLS) regressions to each site, with weights representing 1/propagated error, to provide a predictive model where symmetry about the axes is not required but the uncertainty of each data point is considered.

Due to the meridional gradient between NOG and HYD we do not combine data from both sites in average values. All SSTAs are also calibration specific. Therefore, a range of values is provided for each period in the five-reef sequence, accompanied by ±1 standard deviation of all the corals that date to the given interval.

4.3. Development of the WPWP Coral Sr/Ca-Derived SSTA Compilation

We created a Sr/Ca-derived SSTA compilation with 52 corals from five different regions in the WPWP, including Indonesia, Vanuatu, Papua New Guinea, Tahiti, and the GBR. The coral geochemical proxy results of Gagan et al. (2004) include SSTAs based on coral Sr/Ca from the raised reefs of Vanuatu (Beck et al., 1997; Corrège et al., 2000), Papua New Guinea (McCulloch et al., 1996), Sumba (Pirazzoli et al., 1991), and Alor (Hantoro et al., 1994) in southeastern Indonesia, and the GBR (Gagan et al., 1998, 2002).

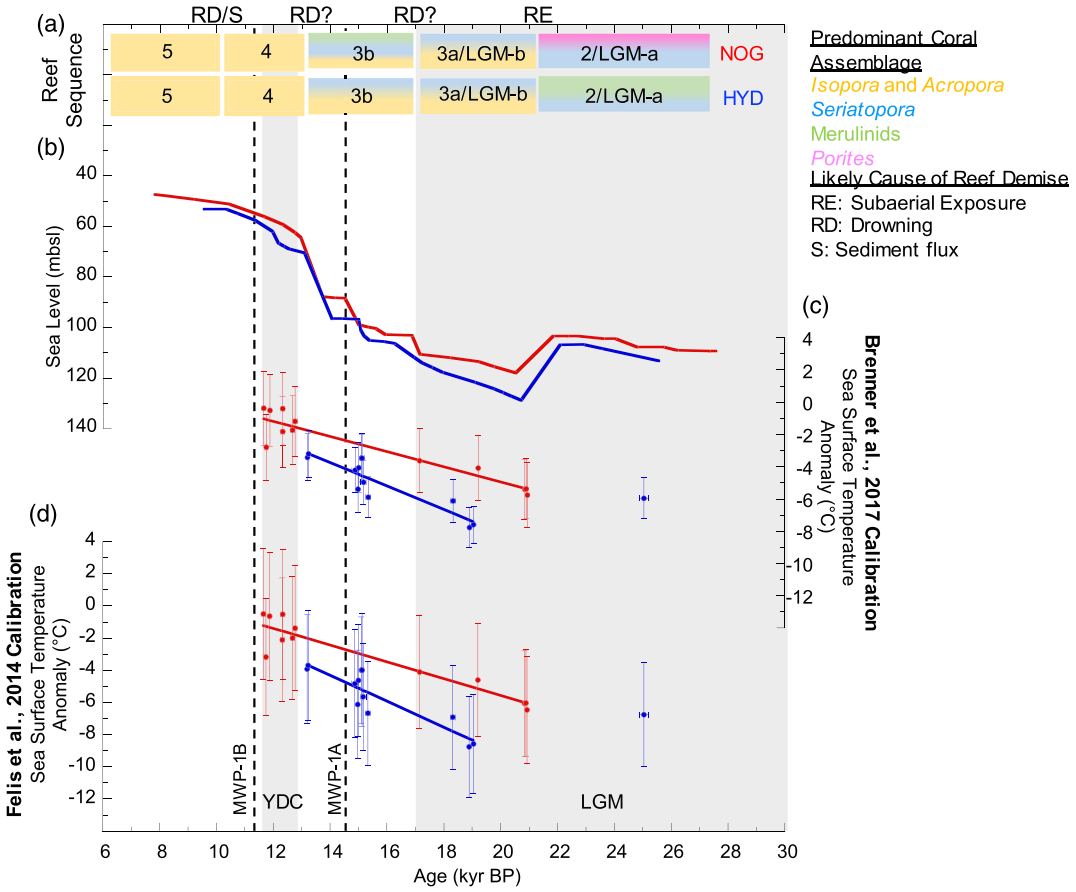

Figure 2. (a) LGM reef sequence for NOG and HYD is outlined with horizontal bars representing duration (see Webster et al., 2018, and Humblet et al., 2019, for details on the reef sequences). The color of each bar refers to the proportion of the dominant coral genera forming the reef's coralgal assemblage. It does not reflect the timing of coralgal assemblage changes within a reef (see Humblet et al., 2019, for further details on the coralgal assemblages). The reason for reef demise is denoted on the upper *X* axis by subaerial reef exposure (RE), reef drowning (RD), or sediment influx (S) (after Webster et al., 2018). (b) Maximum relative sea level history for NOG (red) and HYD (blue) (Yokoyama et al., 2018). (c) Sr/Ca-derived SSTA for NOG (red) and HYD (blue) (Felis et al., 2014) calculated using the Brenner et al. (2017) calibration relative to modern SSTs at each site (this study). (d) Sr/Ca-derived SSTA calculated for NOG (red) and HYD (blue) (Felis et al., 2014) calculated using the Felis et al. (2014) calibration relative to modern SSTs at each site (this study). In panels (c) and (d) the vertical and horizontal error bars denote propagated errors for SSTA and two standard deviations of U-Th ages, respectively. If horizontal error bars are not visible, they are smaller than the marker. The WLS regressions ($p < 0.001$), which are weighted by propagated error, yielded multiple r^2 values of 0.88 (NOG) and 0.81 (HYD). Gray bars denote the LGM as described in Yokoyama et al. (2018) and the YDC. Dashed lines identify the approximate onset of reported Meltwater Pulses (MWP)-1A and MWP-1B (Abdul et al., 2016; Deschamps et al., 2012).

Gagan et al. (2004) recalculated SSTAs for these coral Sr/Ca studies using a single, regional SST calibration, and these values are included in Figure 3. Some of the Gagan et al. (2004) SSTAs were adjusted by Gagan et al. (2012) to account for a potential smoothing effect of calcification in *Porites*, but these values are not included here. Only four SSTAs in this compilation are calculated from GBR corals (Gagan et al., 1998, 2002; Sadler et al., 2016), when excluding the IODP Expeditions 325 GBR corals. See supporting information for further details on these SSTAs. For the purposes of an accurate comparison, we only compared our SSTAs to those that are uncorrected for any potential change in the Sr/Ca of seawater. It is noted on Figure 3 when uncorrected Sr/Ca-based SSTAs are plotted in lieu of any published corrected values.

5. Results

SSTAs for a given reef (Reefs 2 through 4) or time period (e.g., LGM-a) are site-specific, due to the meridional gradient between NOG and HYD, and calibration-specific. A range of calibration-specific SSTAs are

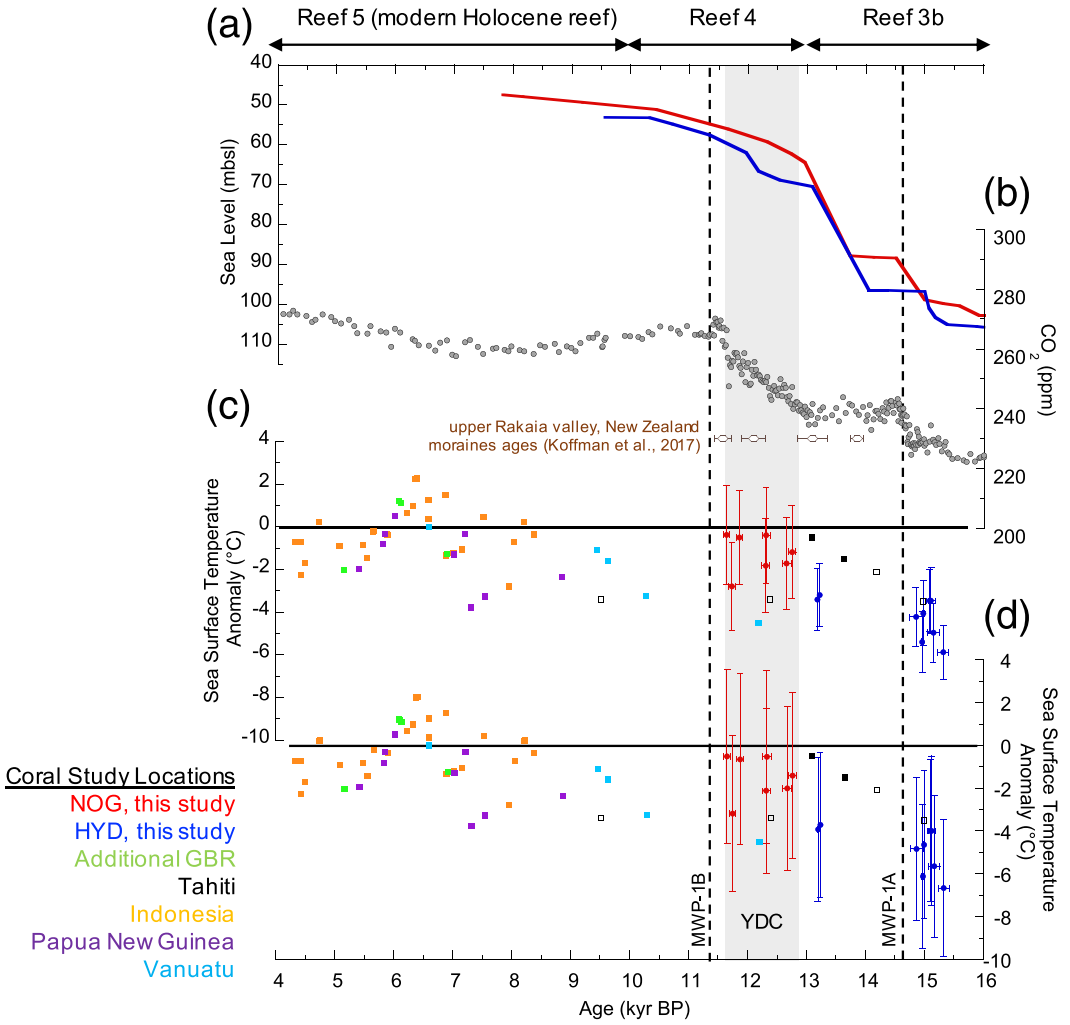

Figure 3. (a) Maximum relative sea level curves for the NOG (red) and HYD (blue) (Yokoyama et al., 2018). (b) Atmospheric CO_2 from Antarctic ice cores (gray circles) (Bereiter et al., 2015) with mean ages for moraine ridges in the upper Rakaia valley, Southern Alps, New Zealand (brown horizontal diamonds; Koffman et al., 2017). (c) Sr/Ca-derived SSTAs for NOG (red) and HYD (blue) Felis et al. (2014) calculated using the Brenner et al. (2017) SST calibration relative to modern SST at each site. The horizontal line represents the 0°C anomaly. (d) Sr/Ca-derived SSTAs for NOG (red) and HYD (blue) calculated using the Felis et al. (2014) SST calibration relative to modern SST at each site. The horizontal line representing the 0°C anomaly. In panels (c) and (d) the vertical and horizontal error bars denote propagated errors for SSTA and two standard deviations of U-Th ages, respectively. If horizontal error bars are not visible they are smaller than the marker. For comparison, in panels (c) and (d) coral-based Sr/Ca-derived SSTAs for the period from 16–4 kyr BP are included for the GBR (light green: Gagan et al., 2004; Sadler et al., 2016), Vanuatu (light blue: Corrège et al., 2004; Duprey et al., 2012; Gagan et al., 2004), Indonesia (yellow: Abram et al., 2009; Gagan et al., 2004), Papua New Guinea (purple: Abram et al., 2009; Gagan et al., 2004), and Tahiti (black: Asami et al., 2009; Cohen & Hart, 2004; DeLong et al., 2010; Felis et al., 2012). All SSTAs are based on data that are uncorrected for potential seawater Sr/Ca composition changes. However, open black squares for Tahiti represent specific studies that also published coral-based SSTAs that were corrected for changes in the Sr/Ca composition of seawater (Asami et al., 2009; DeLong et al., 2010; Felis et al., 2012). The gray bar denotes the YDC. Dashed lines identify the approximate onset of Meltwater Pulses (MWP)-1A and MWP-1B (Abdul et al., 2016; Deschamps et al., 2012).

provided with the first listed value calculated using the Brenner et al. (2017) regression and the second listed value calculated with the Felis et al. (2014) regression. Further, each SSTA is accompanied by ±1 standard deviation of all the corals that date to the given interval. Site- and calibration-specific SSTAs averaged over a reef sequence unit or time period can be found in Table 1. Average conditions for each reef are given in Table 1 and are divided by calibration, site, and reef number. Based on Sr/Ca data, on average, the LGM on the GBR was 4.8 ± 0.9°C to 5.5 ± 1.0°C cooler relative to modern at NOG (n = 5) and 6.9 ± 1.0°C to

Table 1
Site-Specific SSTAs and $\delta^{18}O_{sw}$ ± 1 Standard Deviation With Mean Absolute Error of Propagated Errors in Parentheses, Delineated by Reef Sequence (Webster et al., 2018) and SL-Based LGM Components (Yokoyama et al., 2018)

	Reef 2/LGM-a	Reef 3a/LGM-b	LGM	Reef 3b	Reef 4/YDC	Calibration
Age range (kyr BP)	27–22	21–17	27–17	17–13	13–10	
Number of coral records (NOG/HYD)	0/1	5/3	5/4	0/9	7/0	
Sr/Ca-derived NOG SSTA (°C)	n/a	−4.8 ± 0.9 (1.9)	−4.8 ± 0.9 (1.9)	n/a	−1.3 ± 0.9 (2.2)	Brenner et al. (2017)
	n/a	−5.5 ± 1.0 (3.4)	−5.5 ± 1.0 (3.4)	n/a	−1.5 ± 1.0 (3.9)	Felis et al. (2014)
Sr/Ca-derived HYD SSTA (°C)	−6.0 (1.7)	−7.2 ± 0.9 (1.6)	−6.9 ± 1.0 (1.7)	−4.2 ± 1.0 (1.9)	n/a	Brenner et al. (2017)
	−6.7 (3.1)	−8.1 ± 1.0 (2.9)	−7.8 ± 1.1 (3.0)	−4.8 ± 1.1 (3.3)	n/a	Felis et al. (2014)
δ^{18}O-derived NOG SSTA (°C)	n/a	−8.4 ± 1.0 (1.4)	−8.4 ± 1.0 (1.4)	n/a	−3.8 ± 0.8 (1.8)	Brenner et al. (2017)
	n/a	−6.8 ± 0.9 (3.4)	−6.8 ± 0.9 (3.4)	n/a	−2.9 ± 0.7 (3.7)	Felis et al. (2014)
δ^{18}O-derived HYD SSTA (°C)	−9.9 (1.3)	−10.8 ± 1.0 (1.2)	−10.6 ± 0.9 (1.2)	−7.9 ± 1.2 (1.4)	n/a	Brenner et al. (2017)
	−8.0 (3.2)	−8.8 ± 0.8 (3.1)	−8.6 ± 0.8 (3.2)	−6.3 ± 1.0 (3.4)	n/a	Felis et al. (2014)
NOG δ^{18}Osw (‰)	n/a	0.7 ± 0.1 (0.5)	0.7 ± 0.1 (0.5)	n/a	0.5 ± 0.2 (0.5)	Brenner et al. (2017)
	n/a	0.5 ± 0.1 (1.0)	0.5 ± 0.1 (1.0)	n/a	0.4 ± 0.2 (1.2)	Felis et al. (2014)
HYD δ^{18}Osw (‰)	0.7 (0.4)	0.7 ± 0.1 (0.4)	0.7 ± 0.1 (0.4)	0.7 ± 0.2 (0.5)	n/a	Brenner et al. (2017)
	0.6 (1.0)	0.5 ± 0.1 (1.0)	0.5 ± 0.1 (1.0)	0.6 ± 0.2 (1.1)	n/a	Felis et al. (2014)

Note. Calibration type is noted for each value. SSTAs are reported in °C and seawater values in ‰ (SMOW).

7.8 ± 1.1°C cooler relative to modern at HYD (n = 4) (Figure 2). The LGM can be broken down into two components, LGM-a (i.e., Reef 2) and LGM-b (i.e., Reef 3a). LGM-a was 6.0°C to 6.7°C cooler relative to modern at HYD (n = 1). During LGM-b NOG was 4.8 ± 0.9°C to 5.5 ± 1.0°C cooler relative to modern and HYD was 7.2 ± 0.9°C to 8.1 ± 1.0°C cooler relative to modern (Figure 2). All Reef 3b corals are from HYD (n = 9), yielding an average temperature of 4.2 ± 1.0°C to 4.8 ± 1.1°C cooler than modern. There were no LGM corals from NOG suitable for geochemical analysis. YDC-aged corals are all from NOG (n = 7) and comprise all of Reef 4 in this data set, yielding an average temperature of 1.3 ± 0.9°C to 1.5 ± 1.0°C cooler than modern.

To estimate deglacial warming, the HYD regression omits the oldest sample (25.04 kyr BP) because this coral grew and died prior to deglaciation (i.e., Reef 2). Therefore, the site-specific trends are calculated from samples aged 21 kyr BP and younger. The WLS regressions through Sr/Ca-derived SSTAs returned statistically significant ($p < 0.001$) multiple r^2 values of 0.88 (NOG) and 0.81 (HYD) and indicate that SSTs warmed at a rate of 0.47°C kyr^{-1} (Brenner et al., 2017) to 0.52°C kyr^{-1} (Felis et al., 2014) at NOG and to 0.73°C kyr^{-1} (Brenner et al., 2017) to 0.80°C kyr^{-1} (Felis et al., 2014) at HYD (Figure 2). It is important to keep in mind the various sources of uncertainty associated with the SSTA calculations (see section 4.2) and from this site-specific perspective data are sparse and may be impacted by outliers. These factors reduce the ability of the regressions to model actual conditions, hence, warming rates are estimates.

The δ^{18}O-derived LGM SSTA range from 8.4 ± 1.0°C to 6.8 ± 0.9°C cooler relative to modern at NOG (n = 5) and 10.6 ± 0.9°C to 8.6 ± 0.8°C cooler relative to modern at HYD (n = 4) (Figure 2, Table 1). These values are ~3°C cooler than the Sr/Ca-derived SSTA (Table 1). The Sr/Ca- and δ^{18}O-derived SSTAs cannot both be correct, therefore all further reported SSTAs are based on Sr/Ca measurements, unless otherwise noted. The $\delta^{18}O_{sw}$ record is the result of a consistent positive δ^{18}O anomaly (Table 1). However, there is no significant trend through $\delta^{18}O_{sw}$ at either NOG or HYD. See supporting information for the complete δ^{18}O-derived SSTAs and $\delta^{18}O_{sw}$ records.

6. Discussion

6.1. Understanding Uncertainty in Coral SSTAs

The LGM SSTAs reported here are very similar to those reported in Felis et al. (2014), suggesting that the *Isopora*-based calibrations yield comparable results relative to those calibrated with *Porites*. The propagated error associated with each SSTA considers numerous aspects of uncertainty in the SSTA calculations (Figures 2 and 3). Absolute SST reconstructions from fossil corals like these inherently yield large uncertainties. The thorough accounting of uncertainty via traditional error propagation underscores the need for the paleo-reef community to focus on inferences based on relative SST changes throughout a record, which

might be more meaningful than those based on absolute calculations. In addition to error propagation and outlining the value of relative SST changes, our two-calibration approach provides a range of SSTAs for a robust presentation of conditions on the GBR since the LGM and represent different methodological approaches to SST reconstructions.

One unquantified unknown is the variability in the Sr/Ca composition of seawater over the glacial-interglacial transition. We opted not to correct the SSTAs for potential changes in the Sr/Ca of seawater, due to the multiple uncertainties associated with this process as outlined by Felis et al. (2012). In this case, our SSTAs may provide maximum cooling estimates since some studies suggest that Sr/Ca in seawater was higher during the LGM (e.g., Stoll et al., 1999). Average coral Sr/Ca during the LGM was 9.6 (NOG) and 9.8 (HYD) mmol mol^{-1} and, if we assume that the Sr/Ca of LGM seawater was 1.1% higher than modern (Stoll et al., 1999), corrected values interpreted in the context of our regressions yield SSTAs ~1.3°C (NOG) and ~1.4°C (HYD) warmer than if no adjustment is applied. This adjustment shifts closer to the foraminiferal-derived 2.5s°C cooling during the LGM in the Queensland Trough (de Garidel-Thoron et al., 2004; Dunbar & Dickens, 2003; Jorry et al., 2008) compiled by Reeves, Bostock, et al. (2013). However, even if corrected for potential variability in the Sr/Ca of seawater, both sites produce SSTAs slightly cooler than the ~1°C drop in temperature calculated from foraminiferal proxies in sediment cores in the northern Coral Sea (Anderson et al., 1989; Reeves, Bostock, et al., 2013). The variability in marine-based LGM SSTs signals the need to further focus on this time period on the GBR.

We can add further constraints to our interpretation of maximum cooling during the LGM if we take into consideration the current ecological limit of *Isopora* growth. The southernmost appearance of modern *Isopora* reefs occurs at Lord Howe Island (159.1°E, 31.5°S) where mean annual SST is ~21.5° (Locarnini et al., 2010; Veron & Done, 1979). Therefore, based on the modern SST benchmarks, maximum cooling may have only been ~5°C and ~4.5°C at NOG and HYD, respectively (Felis et al., 2014). While individual *Isopora* may have adapted to thrive in cooler conditions during the deglaciation following the LGM, the modern limit provides a potential constraint to consider and suggests that the propagated error ranges presented here are larger than what is ecologically likely.

6.2. GBR Growth, RSL, and SSTA History Since the LGM

Here we integrate information regarding reef sequence, including vertical accretion rates, coralgal assemblages (Humblet et al., 2019; Webster et al., 2018), RSL (Yokoyama et al., 2018), and our Sr/Ca-derived SSTAs to investigate the evolution of the GBR since the LGM. The beginning of the GBR shelf-edge reef system is marked by the exposure and death of Reef 1 at ~30 kyr BP (Webster et al., 2018), but our record tracks SSTA from Reefs 2 through 4 (Figure 2).

Reef 2 (~28–21 kyr BP) and Reef 3a (~21–17 kyr BP) developed during the LGM (Webster et al., 2011, 2018; Yokoyama et al., 2018). Since the Reef 2 SSTA (i.e., LGM-a) is only based on one coral (HYD) from ~25 kyr BP and since there were no corals from NOG suitable for SSTA analysis, conclusions regarding this period are tenuous. HYD data indicate a possible ~1°C drop in SST from LGM-a (Reef 2) to LGM-b (Reef 3a) with a coincident drop in RSL to its minimum height of ~118 mbsl (Yokoyama et al., 2018). This SST and RSL drop from Reef 2 to 3a is also associated with a coralgal shift from merulinid-rich to acroporid-rich assemblages when shallow-reef growth responded to the RSL minimum by migrating seawards at a rate of 0.2 (NOG) to 0.5 (HYD) m yr^{-1} (Humblet et al., 2019; Webster et al., 2018). More specifically, during Reef 2, in NOG the coral assemblage was comprised mainly of *Acropora*, *Montipora*, and *Porites* and in HYD it was dominated by Merulinidae (e.g., *Dipsastraea, Cyphastrea*, and *Hydnophora*), while during Reef 3a, NOG and HYD were both dominated by *Acropora, Seriatopora*, and *Isopora* (Humblet et al., 2019; Webster et al., 2018). Our new SSTAs support the conclusions of Humblet et al. (2019), which were based on the previous Felis et al. (2014) findings, that peak cooling during the LGM did not preclude the growth of corals that are now dominant in modern GBR reefs (e.g., *Isopora*, *Acropora*). While based on a single SSTA point, it does not appear that SSTA played a major role in the demise of Reef 2, which was subaerially exposed after a rapid RLS fall, or Reef 3a, which can be attributed to RSL rise and an increase in sediment flux to the region (Hinestrosa et al., 2019; Humblet et al., 2019; Webster et al., 2018).

As rising sea level flooded the shelf during the deglacial transition, Reef 3b, which commenced at ~17 kyr BP, thrived as a fringing reef growing on the former site of Reef 2. Reef 3b is also characterized by vertical

accretion rates as high as 20 mm yr^{-1} from 15.5–15 kyr BP (Webster et al., 2018). These rates are the highest in the GBR over the past 30 kyr despite cool SSTAs, only ~2°C (Brenner et al., 2017) to ~3°C (Felis et al., 2014) warmer than temperatures during the LGM on HYD. The Reef 3b assemblage was largely comprised of shallow water, high-energy genera at both sites with coralgal assemblages including *Isopora, Acropora*, with *Seriatopora* and some Merulinidae also present in NOG (Humblet et al., 2019). This mix of genera, particularly the fast-growing *Acropora* and *Isopora* species, could explain how the reef was able to survive rapid sea level rise of 20 mm yr^{-1} (Humblet et al., 2019; Webster et al., 2018; Yokoyama et al., 2018). Reef 3b growth turned off after Meltwater Pulse (MWP) 1-A and prior to the YDC (Webster et al., 2018). Death was likely due to continued sea level rise and increased sediment input negatively impacted water quality (e.g., reduced sunlight penetration, increased nutrients) (Hinestrosa et al., 2016; Webster et al., 2018) exerting more stress on the reef than the cool SSTAs.

Reef 4, the proto-GBR and last reef in the deglacial sequence, developed a typical barrier reef morphology, closely resembling the GBR's modern, shelf structure, with a landward migration of 1.3–1.8 km in less than 2 kyr, following flooding of former Reef 1 (Webster et al., 2018). The Reef 4 assemblage mainly consisted of robustly branching or columnar *Isopora*, with vertical accretion rates up to 9.6 mm yr^{-1} at the reef's onset but dropped off dramatically after ~11.5 kyr BP (Humblet et al., 2019; Webster et al., 2018). RSL climbed ~4 mm yr^{-1} during Reef 4 and reached ~50 mbsl by its turn off at ~10 ka (Webster et al., 2018; Yokoyama et al., 2018). Notably, SSTAs approached modern conditions, 1.3 ± 0.9°C to 1.5 ± 1.0°C cooler than modern. The most important takeaway from our record is that there is clear relative warming during the YDC compared to the LGM (Figure 2).

Based on the assemblage work conducted by Webster et al. (2018) and Humblet et al. (2019), there is no clear drowning event associated with MWP-1B (11.45 ka), which is present in Barbados (Abdul et al., 2016; Bard et al., 1990; Fairbanks, 1989). Instead, the top of Reef 4 is marked by a major slowdown in vertical accretion rates to 4.2 (HYD) to 1.4 (NOG) mm yr^{-1} leading up to its ultimate demise. However, the reason for this change in rate is still uncertain (Webster et al., 2018) and most of the IODP Expedition 325 corals with SSTAs are from the initial growth of Reef 4 (~13–11.7 kyr BP). Webster et al. (2018) proposed that Reef 4 death was due to increased sedimentation, mostly comprised of fine siliclastic and carbonate sediments, which was up to 3 times higher than the deglacial sediment flux (Dunbar et al., 2000; Page & Dickens, 2005), although they could not rule out the influence of reduced calcification (Perry et al., 2012) from increased pCO_2. The sedimentation hypothesis is further supported by the fact that Reef 4 was dominated by *Isopora*, a genus considered to be sediment-intolerant (Blanchon et al., 2014; Kojis & Quinn, 1984; Montaggioni, 2005; Webster et al., 2018). In our study, Reef 4 corals are comprised entirely of YDC-aged samples. Therefore, Reef 4 and YDC are synonymous here, although Reef 4 growth technically ceased following the YDC at ~10 ka (Webster et al., 2018). The turn-on of Reef 5 at ~9 kyr BP, represents the establishment of the modern (Holocene) GBR (Hopley et al., 2007; Humblet et al., 2019; Webster et al., 2018).

In an effort to explore the impact of hydrology and ocean currents since the LGM, we calculated the $\delta^{18}O$ of seawater ($\delta^{18}O_{sw}$). However, the $\delta^{18}O_{sw}$ from each period in the reef sequence are within 1 standard deviation of each other, suggesting that there is little variation. Furthermore, any signal in the $\delta^{18}O_{sw}$ record is swamped by the compounded uncertainties of both the Sr/Ca-derived SST and the $\delta^{18}O$ conversion and therefore does not appear to yield any significant temporal or spatial (e.g., meridional gradient) trend (Figure S2). Here, the exploration of the $\delta^{18}O_{sw}$ did not clearly elucidate the changes in hydrology that other Southern Hemisphere noncoral proxy (e.g., Krause et al., 2019) and modeling studies (e.g., Di Nezio et al., 2016) have identified. Regardless, this is an area that requires further multiproxy investigation to clarify the meaning behind the coral $\delta^{18}O_{sw}$ and hydrologic changes on the GBR since the LGM.

6.3. Significance and Contextualization of YDC Warmth on the GBR

Warming on the GBR during the YDC was identified by Felis et al. (2014), who determined the signal was similar in New Zealand (Bostock et al., 2013; Kaplan et al., 2010) and to the north in the WPWP (Linsley et al., 2010). However, they noted that this warming is in contrast to the only other South Pacific YDC-aged coral-based estimates from Tahiti (Asami et al., 2009) and Vanuatu (Corrège et al., 2004). Although with our propagated uncertainties this disparity is less stark, the GBR SSTAs still support continued warming through the YDC (i.e., Reef 4). Although we were only able to locate two other published fossil corals dating to the

YDC, the seven samples recovered by IODP Expedition 325 indicate that corals of that age do in fact exist in the WPWP during this unique climate interval and signals the need to continue to search for additional coeval corals via scientific drilling.

Water temperature during the YDC on the GBR was similar to today, with an SSTA of 1.3 ± 0.9°C to 1.5 ± 1.0°C cooler than modern. In further examining the YDC-aged corals, the sample dated to 11.746 kyr BP (325-57A-5R-1 (1–3)) is >1.5 standard deviations cooler than the mean during this interval (Figure 3). With the small sample size of YDC-aged corals, it is difficult to establish statistical thresholds to determine outliers. Therefore, this coral cannot be omitted based on available data and although with its inclusion there is no statistically significant YDC trend, we can still consider the average temperature during this interval. As all corals dated to the YDC are from NOG we cannot complete an intersite comparison.

The SSTAs yielded by our YDC-aged corals are not consistently reached at other sites in the WPWP region until 8 kyr BP at the earliest, although Vanuatu corals appear to warm closer to ~9 kyr BP (Figure 3). As previously discussed, we did not adjust our Sr/Ca measurements for potential glacial-interglacial changes in the Sr/Ca composition of seawater. Therefore, our SSTAs likely provide a minimum SSTA for the YDC, which avoids overestimation of the relative warmth during this interval. It is difficult to draw statistically robust conclusions with corals comparing the expression of the YDC on the GBR to other Southern Hemisphere locales as samples dated to this period are rare in the literature. However, we can outline three major takeaways regarding the YDC. First, there is no evidence for cooling on the GBR during the YDC, even when considering our uncertainty estimates. Next, the simple fact that multiple corals that dated to this interval were retrieved signals the possibility that more can be recovered, potentially in other WPWP locations. Scientific reef coring efforts that focus on the YDC could resolve some of the geographic heterogeneity and fill in the current spatial and temporal data gaps. Finally, modern temperatures appear to be reached on the GBR during the YDC and approach the values recorded in other early Holocene corals throughout the WPWP. With the limited available data, from a qualitative standpoint the GBR appears warmer that other parts of the WPWP (Figure 3). Aside from the small sample size limiting the YDC comparison, we should consider that zonal SST gradients could influence the intersite temperature offset.

6.4. Potential YDC-Warmth Mechanisms

The mechanisms behind the Northern and Southern Hemispheres expression of the YDC are continually being explored. Understanding the drivers behind the warming in the Southern Hemisphere during this interval will likely lead to a deeper understanding of its apparent geographic heterogeneity. For this reason, it should be considered whether multiple processes resulted in YDC warming on the GBR.

The steeper meridional SST gradient along the GBR during the LGM and deglaciation weakened after 12.7 kyr BP as HYD warmed to a greater degree than NOG (Felis et al., 2014). Felis et al. (2014) suggested that this was potentially the result of a strengthening subtropical Pacific gyre and EAC (Bostock et al., 2006). But the climate mechanisms responsible for 2–3°C greater warming during the YDC on the GBR compared to fossil evidence at Vanuatu (Corrège et al., 2004) and Tahiti (Asami et al., 2009) is unclear. Note that all Sr/Ca-SSTA values discussed here are uncorrected for Sr/Ca-seawater composition changes, although Asami et al. (2009) provide options for corrected SSTAs in their study. However, if all values were adjusted, they would all shift to yield warmer conditions with the relative difference between the sites preserved. The very limited amount of YDC-aged fossil coral data in the South Pacific prohibits a more critical evaluation of specific mechanisms. At face value, the GBR, Vanuatu, and Tahiti YDC results suggest that the GBR warmed more than the central and southwestern South Pacific at this time. Perhaps the strength of the EAC on millennial time scales is controlled more by the Southern Hemisphere subtropical front along the edge of the Southern Ocean (~43°S) (SF in Figure 1) and less by gyre strength as proposed by Strand et al. (2019, and references therein). This might explain the relatively warm conditions on the GBR during the YDC. A change in the mean position of the South Pacific Convergence Zone (SPCZ) during the YDC could also explain relative cooling in the central SW Pacific gyre region. Today, a more zonal orientation and equatorial location of the SPCZ results in the cooler (and saltier) conditions in a broad region including Tahiti and Vanuatu (Linsley et al., 2017; Vincent et al., 2009). While we cannot distinguish the relative importance of each mechanism, we speculate that at least the GBR and New Zealand are influenced by the same or related

regional drivers. This is based on proximity and the similar timing of warming at both sites that appears to coincide with an increase in atmospheric CO_2 in New Zealand glaciers (e.g., Kaplan et al., 2010; Koffman et al., 2017; Strand et al., 2019).

In the upper Rakaia Valley of New Zealand, glacier-inferred temperatures were about 1°C cooler than modern from ~13.140–11.620 ka (Koffman et al., 2017), comparable to the temperatures at NOG and HYD. The glacial retreat in New Zealand, during Northern Hemisphere Heinrich Stadials (e.g., Heinrich Stadial 1 and Heinrich Stadial 0/YDC) (Koffman et al., 2017; Strand et al., 2019) is paralleled by warming in the Chilean Lake District (Denton et al., 1999; Moreno et al., 2015). Strand et al. (2019) suggested that this pan-Pacific signal during the YDC is due to either atmospheric or oceanic transport of heat leading to southerly shifts in the thermal equator coinciding with winter-centric Heinrich Stadials. In turn, this pushes the Southern Hemisphere westerlies, the Australasian monsoon system, and the Subtropical front at the northern edge of the Southern Ocean southward (Chiang et al., 2009; Strand et al., 2019). These shifts require the bipolar seesaw (Timmerman et al., 2007), which allows North Atlantic circulation and increased heat sequestration in the Southern Ocean via deepwater formation. This leads to enhanced Southern Ocean upwelling and degassing of CO_2 (Anderson et al., 2009).

The evolution of atmospheric CO_2 since the LGM is also correlated to moraine-based late glacial warming observations (e.g., Kaplan et al., 2010; Koffman et al., 2017; Strand et al., 2019). This air temperature-CO_2 relationship is consistent with a compilation of foraminiferal-based SST records throughout the IPWP (South China Sea: Moffa-Sanchez et al., 2019, Steinke et al., 2008, 2011, Sumatra: Mohtadi et al., 2014, Papua New Guinea: Moffa-Sanchez et al., 2019, Timor Sea: Gibbons et al., 2014; Holbourn et al., 2011; Levi et al., 2007; Xu et al., 2008, and the Indonesian Throughflow: Fan et al., 2013; Linsley et al., 2010; Rosenthal et al., 2003; Schröder et al., 2016, 2018; Stott et al., 2004) (Moffa-Sanchez et al., 2019). The coevolution of SST and CO_2 is also evident in our SSTA record when corals record near modern temperatures during the YDC and there is a coincident rise in atmospheric CO_2 commencing around 12 kyr BP (Bereiter et al., 2015) (Figure 3).

There is additional potential evidence in Antarctica for warming during the YDC. Following its retreat from its maximum LGM position, the grounding line of the paleo-Bindschadler Ice Stream stabilized ~14.7 cal. (calibrated) kyr BP, indicated by radiocarbon ages of benthic foraminifera (Bart et al., 2018). This ice sheet collapsed after ~12.3 cal. kyr BP and the grounding line was stable until ~11.5 cal. kyr BP (Bart & Tulaczyk, 2020). However, shortly after, and potentially synchronous with, MWP-1B a rapid 200 km ice retreat was recorded in the Ross Sea (Bart et al., 2018). The timing of this Antarctic ice sheet retreat occurs at the end of the YDC, and we speculate that this could be related to synchronous YDC warming apparent on the GBR.

The exact reasons for the shifts in the climate system that lead to YDC warming on the GBR are still uncertain, as indicated by modeling studies. The YDC's Northern Hemisphere expression is reconstructed well by simulating the draining of the massive glacial Lake Agassiz leading to a shutdown of Atlantic Meridional Overturning Circulation (AMOC) (Manabe & Stouffer, 1997). However, it fails to recreate the warming that we now know is present in the Southern Hemisphere. Renssen et al. (2015) performed experiments with the LOVECLIM model to identify the driver, or drivers, behind the YDC that would result in hemispheric SST asymmetry. Some combination of a significant reduction in AMOC, atypical atmospheric northerly flow over Europe, and some moderate measure of radiative cooling due to either increased atmospheric dust or a decrease in atmospheric methane or nitrous oxide were necessary for them to reproduce YDC conditions with hemispheric bipolarity (Renssen et al., 2015), even with global CO_2 rising. However, they were unable to disentangle the relative significance of each forcing. Our coral SSTA record underscores the need to further investigate the YDC throughout the GBR and Indo-Pacific to further clarify the global heterogeneity of deglacial millennial climate variability and improve comparisons of model output. It is imperative to consider the growing compendium of proxy-based results from the Southern Hemisphere in revised model experiments to more fully outline potential drivers and their relative importance.

6.5. Significance of Reef 4 and Implications for the Future

A full understanding of the demise of GBR Reef 4 is critical since its near modern barrier reef morphology provides an opportunity to explore the limits of GBR's development prior to anthropogenic influence. It is likely that SST rise, exceeding a certain threshold temperature and/or warming rate, in conjunction with

other stressors, like sedimentation, make reefs vulnerable to drowning as a result of slowing vertical accretion. As discussed earlier, Webster et al. (2018) determined that Reef 4's demise could not solely be attributed to rising sea level but instead was driven by a combination of sea level and a massive influx of sediment to the region. Absolute temperature is not what typically leads to coral bleaching and potential subsequent coral death, but instead the rate of change or sustained exceedance of mean monthly maximum temperatures normally experienced at a given site (i.e., degree heating weeks) is often the culprit (e.g., Hughes et al., 2017). It is possible that the SST conditions during the YDC (see sections 6.2 and 6.3) may have contributed to slowing vertical accretion and further destabilized the reef ecosystem.

With sea and air temperatures rising, the biological, physical, and chemical integrity of the GBR are at great risk in the coming decades (Lough, 2007). According to Representative Concentration Pathway (RCP) 4.5 modeling, bleaching in the GBR will occur at least twice per decade beginning in 2018 with conditions conducive to annual bleaching starting between 2052 and 2067 (Moss et al., 2010; van Hooidonk et al., 2013). It is predicted that the SSTs will increase by about 2.5°C by 2100 off the northeastern coast of Australia in the GBR (Cai et al., 2014; Hoegh-Guldberg et al., 2014; Lough et al., 2012; Reisinger et al., 2014; Rhein et al., 2013), ~2 orders of magnitude faster than the rate of warming during the last deglaciation.

The impacts of recurrent bleaching events (i.e., damage to already stressed reefs) has been an important research area for climate scientists, paleoclimatologists, and reef ecologists. Some studies indicate that thermal exposure activates various mechanisms that lead to coral and coral symbiont acclimatization or adaptation to bleaching (e.g., Ainsworth et al., 2016; Bay et al., 2016; Torda et al., 2017) or an increase in the proportion of more heat resistant coral colonies (e.g., Baker et al., 2008). Other work found that there is a cumulative impact of high-frequency mass bleaching events especially when there is insufficient time for more mature coral colonies to grow (Hughes et al., 2017). What is known, however, is that we cannot examine the impact of a given climate-related event on a reef in isolation and must consider the environmental conditions prior to and following the incident of concern for a thorough assessment (Hughes et al., 2019). Although the projected future warming is unprecedented in the context of the LGM and last deglaciation, our paleo data illustrate that a confluence of factors, including SST, can lead to the demise of a reef, supporting the idea that an already weakened system may be more sensitive to additional stressors that may otherwise not have led to reef growth turn off.

7. Conclusions

This IODP Expedition 325 deglacial SSTA record sheds light on the SST history of the GBR with the first application of *Isopora*-based SST calibrations to *Isopora* fossil corals. The GBR was 4.8 $\pm$ 0.9°C to 5.5 $\pm$ 1.0°C cooler relative to modern at NOG ($n = 5$) and 6.9 $\pm$ 1.0°C to 7.8 $\pm$ 1.1°C cooler relative to modern at HYD ($n = 4$) during the LGM. The existing data suggest warming continued through the deglaciation following the LGM. As first noted by Felis et al. (2014), warming on the GBR during the YDC is clear and there is no indication of cooling. These coral data are in line with the growing compendium of moraine-based studies that report warming during the YDC in Southern Hemisphere. The temperature conditions on the GBR during the YDC are not consistently reached at other sites in the WPWP until ~8 kyr BP. Importantly, the mere presence of the many YDC-aged corals indicates that future investigation of this interval is possible, and could clarify some of the spatial differences. By compiling SSTAs with RSL and reef sequence we provide a robust overview of the GBR evolution from the LGM to the base of the Holocene. From this comprehensive perspective, it is clear that the reason for reef stress and demise is multi-factorial. As we consider the future of the GBR and other coral reefs we must consider not only temperature but also the confluence of associated changes in sediment flux, sea level, and existing coralgal assemblage among others for accurate predictions.

Data Availability Statement

Data in this study can be found at https://www.ncdc.noaa.gov/paleo/study/31835 on the NOAA NCEI database and coral geochemical data originally published at https://doi.pangaea.de/10.1594/PANGAEA.833408 on the World Data Center PANGAEA.

Acknowledgments

We are grateful for the three anonymous reviewers who provided incredibly thorough and thoughtful comments on this manuscript. We acknowledge the International Ocean Discovery Program (IODP) and the European Consortium for Ocean Research Drilling (ECORD) for drilling the Great Barrier Reef, and the IODP Bremen Core Repository (BCR) for organizing the onshore sampling party. This research interpreted samples provided by IODP, drilled on a mission-specific platform expedition (Expedition 325—Great Barrier Reef Environmental Changes) conducted by the ECORD Science Operator (ESO). This work was funded by National Science Foundation (NSF) award OCE 13-56948 to B. K. L, with NSF GRFP support DGE-11-44155 to L. D. B., and the Australian Research Council (grant no. DP1094001) and ANZIC IODP. Partial support for B. K. L's work on this project also came from the Vetlesen Foundation via a gift to the Lamont-Doherty Earth Observatory. T. F. received funding from the Deutsche Forschungsgemeinschaft (DFG, German Research Foundation)—Project number 180346848, through Priority Program 527 "IODP." A. T. received support from the UK Natural Environment Research Council (NE/H014136/1 and NE/H014268/1). M. T. thanks Ministry of Earth Sciences for support (NCPOR contribution no. J-84/2020-21). L. D. B. would also like to thank Kassandra Costa for her input regarding error analysis.

References

Abdul, N. A., Mortlock, R. A., Wright, J. D., & Fairbanks, R. W. (2016). Younger Dryas Sea level and meltwater pulse 1B recorded in Barbados reef crest coral *Acropora palmata*. *Paleoceanography*, *31*, 330–344. https://doi.org/10.1002/2015PA002847

Abram, N. J., McGregor, H. V., Gagan, M. K., Hantoro, W. S., & Suwargadi, B. W. (2009). Oscillations in the southern extent of the Indo-Pacific warm pool during the mid-Holocene. *Quaternary Science Reviews*, *28*(25–26), 2794–2803. https://doi.org/10.1016/j.quascirev.2009.07.006

Ainsworth, T. D., Heron, S. F., Ortiz, J. C., Mumby, P. J., Grech, A., Ogawa, D., et al. (2016). Climate change disables coral bleaching protection on the Great Barrier Reef. *Science*, *352*(6283), 338–342. https://doi.org/10.1126/science.aac7125

Anderson, D. M., Prell, W. L., & Barratt, N. J. (1989). Estimates of sea surface temperature in the Coral Sea at the Last Glacial Maximum. *Paleoceanography*, *4*(6), 615–627. https://doi.org/10.1029/PA004i006p00615

Anderson, R. F., Ali, S., Bradtmiller, L. I., Nielsen, S. H., Fleisher, M. Q., Anderson, B. E., & Burckle, L. H. (2009). Wind-driven upwelling in the Southern Ocean and the deglacial rise in atmospheric CO_2. *Science*, *323*(5920), 1443–1448. https://doi.org/10.1126/science.1167441

Andres, M. S., Bernasconi, S. M., McKenzie, J. A., & Rohl, U. (2003). Southern Ocean deglacial record supports global Younger Dryas. *Earth and Planetary Science Letters*, *216*(4), 515–524. https://doi.org/10.1016/S0012-821X(03)0056-9

Asami, R., Felis, T., Deschamps, P., Hanawa, K., Iryu, Y., Bard, E., et al. (2009). Evidence for tropical South Pacific climate change during the younger Dryas and the Bølling-Allerød from geochemical records of fossil Tahiti corals. *Earth and Planetary Science Letters*, *288*(1–2), 96–107. https://doi.org/10.1016/j.epsl.2009.09.011

Baker, A. C., Glynn, P. W., & Riegl, B. (2008). Climate change and coral reef bleaching: An ecological assessment of long-term impacts, recovery trends and future outlook. *Estuarine, Coastal and Shelf Science*, *80*(4), 435–471. https://doi.org/10.1016/j.ecss.2008.09.003

Bard, E., Hamelin, B., & Fairbanks, R. G. (1990). U-Th obtained by mass spectrometry in corals from Barbados: Sea level during the past 130,000 years. *Nature*, *346*(6283), 456–458. https://doi.org/10.1038/346456a0

Barrows, T. T., Lehman, S. J., Fifield, L. K., & de Deckker, P. (2007). Absence of cooling in New Zealand and the adjacent ocean during the Younger Dryas Chronozone. *Science*, *318*(5847), 86–89. https://doi.org/10.1126/science.1145873

Bart, P. J., DeCesare, M., Rosenheim, B. E., Majewski, W., & McGlannan, A. (2018). A centuries-long delay between a paleo-ice-shelf collapse and grounding-line retreat in the Whales Deep Basin, eastern Ross Sea, Antarctica. *Scientific Reports*, *8*(1), 12392. https://doi.org/10.1038/s41598-018-29911-8

Bart, P. J., & Tulaczyk, S. (2020). A significant acceleration of ice volume discharge preceded a major retreat of a West Antarctic paleo-ice stream. *Geology*, *48*(4), 313–317. https://doi.org/10.1130/G46916.1

Bay, L. K., Doyle, J., Logan, M., & Berkelmans, R. (2016). Recovery from bleaching is mediated by threshold densities of background thermos-tolerant symbiont types in a reef-building coral. *Royal Society Open Science*, *3*(6), 160322. https://doi.org/10.1098/rsos.160322

Beck, J. W., Récy, J., Taylor, F., Edwards, R. L., & Cabioch, G. (1997). Abrupt changes in early Holocene tropical sea surface temperature derived from coral records. *Nature*, *385*(6618), 705–707. https://doi.org/10.1038/385705a0

Bereiter, B., Eggleston, S., Schmitt, J., Nehrbass-Ahles, C., Stocker, T. F., Fischer, H., et al. (2015). Revision of the EPICA dome C CO_2 record from 800-600 kyr before present. *Geophysical Research Letters*, *42*, 542–549. https://doi.org/10.1002/2014GL61957

Bevington, P., & Robinson, D. K. (2002). *Data reduction and error analysis for the physical science* (3rd ed.). New York: McGraw-Hill Education.

Blanchon, P., Granados-Corea, M., Abbey, E., Braga, J. C., Braithwaite, C., Kennedy, D. M., et al. (2014). Postglacial fringing-reef to barrier-reef conversion on Tahiti links Darwin's reef types. *Scientific Reports*, *4*(1), 4997. https://doi.org/10.1038/srep04997

Bostock, H. C., Barrows, T. T., Carter, L., Chase, Z., Cortese, G., Dunbar, G. B., et al. (2013). A review of the Australian-New Zealand sector of the Southern Ocean over the last 30 ka (Aus-INTIMATE project). *Quaternary Science Reviews*, *74*, 35–57. https://doi.org/10.1016/j.quascirev.2012.07.018

Bostock, H. C., Opdyke, B. N., Gagan, M. K., Kiss, A. E., & Fifield, L. K. (2006). Glacial/interglacial changes in the East Australian current. *Climate Dynamics*, *26*(6), 645–659. https://doi.org/10.1007/s00382-005-0103-7

Brenner, L. D., Linsley, B. K., & Potts, D. C. (2017). A modern Sr/Ca-δ^{18}O- sea surface temperature calibration for *Isopora* corals on the Great Barrier Reef. *Paleoceanography*, *32*, 182–194. https://doi.org/10.1002/2016PA002973

Cai, W., Borlace, S., Lengaigne, M., van Rensch, P., Collins, M., Vecchi, G., et al. (2014). Increasing frequency of extreme El Niño events due to greenhouse warming. *Nature Climate Change*, *4*(2), 111–116. https://doi.org/10.1038/nclimate2100

Chiang, J. C. H., Fang, Y., & Chang, P. (2009). Pacific climate change and ENSO activity in the mid-Holocene. *Journal of Climate*, *22*(4), 923–939. https://doi.org/10.1175/2008JCLI2644.1

Clark, P. U., Pisias, N. G., Stocker, T. F., & Weaver, A. J. (2002). The role of thermohaline circulation in abrupt climate change. *Nature*, *415*(6874), 863–869. https://doi.org/10.1038/415863a

Cohen, A. L., & Hart, S. R. (2004). Deglacial Sea surface temperatures of the western tropical Pacific: A new look at old coral. *Paleoceanography*, *19*, PA4031. https://doi.org/10.1029/2004PA001084

Corrège, T., Delcroix, T., Recy, J., Beck, W., Cabioch, G., & le Cornec, F. (2000). Evidence for stronger El Niño-Southern Oscillation (ENSO) events in a mid-Holocene massive coral. *Paleoceanography*, *14*, 465–470.

Corrège, T., Gagan, M. K., Beck, J. W., Burr, G. S., Cabioch, G., & Le Cornec, F. (2004). Interdecadal variation in the extent of South Pacific tropical waters during the Younger Dryas event. *Nature*, *428*(6986), 927–929. https://doi.org/10.1038/nature02506

Davies, P. J., Symonds, P. A., Feary, D. A., & Pigram, C. J. (1989). The evolution of the carbonate platforms of northeast Australia. In P. D. Crevello, J. L. Wilson, J. F. Sarg, J. F. Read (Eds.), *Controls on carbonate platform and basin development* (Vol. 44, pp. 233–258). Tulsa, OK: Special Publication-Society of Economic Paleontology and Mineralogy. https://doi.org/10.2110/pec.89.44.0233

De Deckker, P., Moros, M., Perner, K., & Jansen, E. (2012). Influence of the tropics and southern westerlies on glacial interhemispheric asymmetry. *Nature Geoscience*, *5*(4), 266–269. https://doi.org/10.1038/ngeo1431

de Garidel-Thoron, T., Beaufort, L., Bassinot, F., & Henry, P. (2004). Evidence for large methane releases to the atmosphere from deep-sea gas-hydrate dissociation during the last glacial episode. *Proceedings of the National Academy of Sciences*, *101*(25), 9187–9192. https://doi.org/10.1073/pnas.0402909101

DeLong, K. L., Quinn, T. M., & Taylor, F. (2010). A snapshot of climate variability at Tahiti at 9.5 ka using a fossil coral from IODP expedition 310. *Geochemistry, Geophysics, Geosystems*, *11*, Q06005. https://doi.org/10.1029/2009GC002758

Denton, G. H., Lowell, T. V., Heusser, C. J., Schlüchter, C., Andersen, B. G., Heusser, L. E., et al. (1999). Geomorphology, stratigraphy, and radiocarbon chronology of Llanquihue drift in the area of the southern Lake District, Seno Reloncavi, and Isla Grande de Chiloe, Chile. *Geografiska Annaler. Series A, Physical Geography*, *81*(2), 167–229.

Deschamps, P., Durand, N., Bard, E., Hamelin, B., Camoin, G., Thomas, A. L., et al. (2012). Ice-sheet collapse and sea-level rise at the Bølling warming 14,600 year ago. *Nature*, *483*(7391), 559–564. https://doi.org/10.1038/nature10902

Di Nezio, P. N., Timmerman, A., Tierney, J. E., Jin, F. -F., Otto-Bliesner, B., Rosenbloom, N., et al. (2016). The climate response of the Indo-Pacific warm pool to glacial sea level. *Paleoceanography*, *31*, 866–894. https://doi.org/10.1002/2015PA002890

Dunbar, G. B., & Dickens, G. R. (2003). Late Quaternary shedding of shallow-marine carbonate along a tropical mixed siliciclastic-carbonate shelf: Great Barrier Reef, Australia. *Sedimentology*, *50*(6), 1061–1077. https://doi.org/10.1046/j.1365-3091.2003.00593.x

Dunbar, G. B., Dickens, G. R., & Carter, R. M. (2000). Sediment flux across the Great Barrier Reef shelf to the Queensland Trough over the last 300 ky. *Sedimentary Geology*, *133*(1–2), 49–92. https://doi.org/10.1016/S0037-0738(00)00027-0

Duprey, N., Lazareth, C. E., Corrège, T., Le Cornec, F., Maes, C., Pujol, N., et al. (2012). Early mid-Holocene SST variability and surface-ocean water balance in the Southwest Pacific. *Paleoceanography*, *27*, PA4207. https://doi.org/10.1029/2012PA002350

Fairbanks, R. (1989). A 17,000-year glacio-eustatic sea level record: Influence of glacial melting rates on the Younger Dryas event and deep-ocean circulation. *Nature*, *342*(6250), 637–642. https://doi.org/10.1038/342637a0

Fan, W., Jian, Z., Bassinot, F., & Chu, Z. (2013). Holocene centennial-scale changes of the Indonesian and South China Sea throughflows: Evidences from the Makassar Strait. *Global and Planetary Change*, *111*, 111–117. https://doi.org/10.1016/j.gloplacha.2013.08.017

Felis, T., McGregor, H. V., Linsley, B. K., Tudhope, A. W., Gagan, M. K., Suzuki, A., et al. (2014). Intensification of the meridional temperature gradient in the Great Barrier Reef following the Last Glacial Maximum. *Nature Communications*, *5*(1), 4102. https://doi.org/10.1038/ncomms5102

Felis, T., Merkel, U., Asami, R., Deschamps, P., Hathorne, E. C., Kölling, M., et al. (2012). Pronounced interannual variability in tropical South Pacific temperatures during Heinrich Stadial 1. *Nature Communications*, *3*(1), 965. https://doi.org/10.1038/ncomms1973

Felis, T., Suzuki, A., Kuhnert, H., Dima, M., Lohmann, G., & Kawahata, H. (2009). Subtropical coral reveals abrupt early-twentieth-century freshening in the western North Pacific Ocean. *Geology*, *37*(6), 527–530. https://doi.org/10.1130/g25581a.1

Gagan, M. K., Ayliffe, L. K., Hopley, D., Cali, J. A., Mortimer, G. E., Chappell, J., et al. (1998). Temperature and surface-ocean water balance of the mid-Holocene tropical western Pacific. *Science*, *279*(5353), 1014–1018. https://doi.org/10.1126/science.279.5353.1014

Gagan, M. K., Ayliffe, L. K., Opdyke, B. N., Hopley, D., Scott-Gagan, H., & Cowley, J. (2002). Coral oxygen isotope evidence for recent groundwater fluxes to the Australian Great Barrier Reef. *Geophysical Research Letters*, *29*(20), 1982. https://doi.org/10.1029/2002GL015336

Gagan, M. K., Dunbar, G. B., & Suzuki, A. (2012). The effect of skeletal mass accumulation in *Porites* on coral Sr/Ca and $\delta^{18}O$ paleothermometry. *Paleoceanography*, *27*, PA1203. https://doi.org/10.1029/2011PA002215

Gagan, M. K., Hendy, E. J., Haberle, S. G., & Hantoro, W. S. (2004). Post-glacial evolution of the Indo-Pacific warm pool and El Niño-Southern Oscillation. *Quaternary International*, *118–119*, 127–143. https://doi.org/10.1016/S1040-6182(03)00134-4

Gibbons, F. T., Oppo, D. W., Mohtadi, M., Rosenthal, Y., Cheng, J., Liu, Z., & Linsley, B. K. (2014). Deglacial $\delta^{18}O$ and hydrologic variability in the tropical Pacific and Indian Oceans. *Earth and Planetary Science Letters*, *387*, 240–251. https://doi.org/10.1016/j.epsl.2013.11.032

Hantoro, W. S., Pirazzoli, P. A., Jouannic, C., Faure, H., Hoang, C. T., Radtke, U., et al. (1994). Quaternary uplifted coral terraces on Alor Island, east Indonesia. *Coral Reefs*, *13*(4), 215–223. https://doi.org/10.1007/BF00303634

Hathorne, E. C., Gagnon, A., Felis, T., Adkins, J., Asami, R., Boer, W., et al. (2013). Interlaboratory study for coral Sr/Ca and other element/Ca ratio measurements. *Geochemistry, Geophysics, Geosystems*, *14*, 3730–3750. https://doi.org/10.1002/ggge.20230

Hewitt, G. (2000). The genetic legacy of the Quaternary ice ages. *Nature*, *405*(6789), 907–913. https://doi.org/10.1038/35016000

Hinestrosa, G., Webster, J. M., & Beaman, R. J. (2016). Postglacial sediment deposition along a mixed carbonate-siliclastic margin: New constraints from the drowned shelf-edge reefs of the Great Barrier Reef, Australia. *Palaeogeography, Palaeoclimatology, Palaeoecology*, *446*, 168–185. https://doi.org/10.1016/j.palaeo.2016.01.023

Hinestrosa, G., Webster, J. M., & Beaman, R. J. (2019). Spatio-temporal patterns in the postglacial flooding of the Great Barrier Reef shelf, Australia. *Continental Shelf Research*, *173*, 13–26. https://doi.org/10.1016/j.csr.2018.12.001

Hoegh-Guldberg, O., Cai, R., Poloczanska, E. S., Brewer, P. G., Sundby, S., Hilmi, K., et al. (2014). The ocean. In V. R. Barros, et al. (Eds.), *Climate change 2014: Impacts, adaptation, and vulnerability. Part B: Regional aspects. Contribution of Working Group II to the Fifth Assessment Report of the Intergovernmental Panel on Climate Change* (Chap. 30, pp. 1655–1731). Cambridge, UK and New York, NY, USA: Cambridge University Press.

Holbourn, A., Kuhnt, W., & Xu, J. (2011). Indonesian throughflow variability during the last 140 ka: The Timor Sea outfliw. *Geological Society, London, Special Publications*, *355*(1), 283–303. https://doi.org/10.1144/SP355.14

Hopley, D., Smithers, S. G., & Parnell, K. E. (2007). *The geomorphology of the Great Barrier Reef: Development, diversity, and change*. USA: Cambridge University Press. https://doi.org/10.1017/CBO9780511535543

Hughes, T., Kerry, J., Álvarez-Noriega, M., Álvarez-Romero, J. G., Anderson, K. D., Baird, A. H., et al. (2017). Global warming and recurrent mass bleaching of corals. *Nature*, *543*, 373–377. https://doi.org/10.1038/nature21707

Hughes, T. P., Kerry, J. T., Connolly, S. R., Baird, A. H., Eakin, C. M., Heron, S. F., et al. (2019). Ecological memory modifies the cumulative impact of recurrent climate extremes. *Nature Climate Change*, *9*(1), 40–43. https://doi.org/10.1038/s41558-018-0351-2

Humblet, M., Potts, D. C., Webster, J. M., Braga, J. C., Iryu, Y., Yokoyama, Y., et al. (2019). Late glacial to deglacial variation of coralalgal assemblages in the Great Barrier Reef, Australia. *Global and Planetary Change*, *174*, 70–91. https://doi.org/10.1016/j.gloplacha.2018.12.014

Humblet, M., & Webster, J. M. (2017). Coral community changes in the great barrier reef in response to major environmental changes over glacial-interglacial timescales. *Palaeogeography, Palaeoclimatology, Palaeoecology*, *472*, 216–235. https://doi.org/10.1016/j.palaeo.2017.02.003

Jorry, S., Droxler, A. W., Mallarino, C., Dickens, G. R., Bentley, S. J., Beaufort, L., et al. (2008). Bundled turbidite deposition in the central Pandora trough (Gulf of Papua) since Last Glacial Maximum: Linking sediment nature and accumulation to sea level fluctuations at millennial timescale. *Journal of Geophysical Research*, *113*, F01S19. https://doi.org/10.1029/2006JF000649

Kaplan, M. R., Schaefer, J. M., Denton, G. H., Barrell, D. J. A., Chinn, T. J. H., Putnam, A. E., et al. (2010). Glacier retreat in New Zealand during the younger Dryas stadial. *Nature*, *467*(7312), 194–197. https://doi.org/10.1038/nature09313

Kaplan, M. R., Schaefer, J. M., Denton, G. H., Doughty, A. M., Barrell, D. J. A., Chinn, T. J. H., et al. (2013). The anatomy of long-term warming since 15 kyr ago in New Zealand based on net glacier snowline rise. *Geology*, *41*(8), 887–890. https://doi.org/10.1130/G34288.1

Kelley, S. E., Kaplan, M. R., Schaefer, J. M., Andersen, B. G., Barrell, D. J. A., Putnam, A. E., et al. (2014). High-precision ^{10}Be chronology of moraines in the southern Alps indicates synchronous cooling in Antarctica and New Zealand 42,000 years ago. *Earth and Planetary Science Letters*, *405*, 194–206. https://doi.org/10.1016/j.epsl.2014.07.031

Koffman, T. N. B., Schaefer, J. M., Putnam, A. E., Denton, G. H., Barrell, D. J. A., Rowan, A. V., et al. (2017). A beryllium-10 chronology of late-glacial moraines in the upper Rakaia valley, southern Alps, New Zealand supports Southern-Hemisphere warming during the Younger Dryas. *Quaternary Science Reviews*, *170*, 14–25. https://doi.org/10.1016/j.quatscirev.2017.06.012

Kojis, B. L., & Quinn, N. J. (1984). Seasonal and depth variation in fecundity of *Acropora palifers* at two reefs in Papua New Guinea. *Coral Reefs*, *3*(3), 165–172. https://doi.org/10.1007/BF00301961

Krause, C. E., Gagan, M. K., Dunbar, G. B., Hantoro, W. S., Hellstrom, J. C., Cheng, J., et al. (2019). Spatio-temporal evolution of Australasian monsoon hydroclimate over the last 40,000 years. *Earth and Planetary Science Letters*, *513*, 103–112. https://doi.org/10.1016/j.epsl.2019.01.045

Levi, C., Labeyrie, L., Bassinot, F., Guichard, F., Cortijo, E., Waelbroeck, C., et al. (2007). Low-latitude hydrological cycle and rapid climate changes during the last deglaciation. *Geochemistry, Geophysics, Geosystems*, *8*, Q05N12. https://doi.org/10.1029/2006GC001514

Linsley, B. K., Dunbar, R. B., Lee, D., Tangri, N., & Dassié, E. P. (2017). Abrupt northward shift of SPCZ position in the late-1920s indicates coordinate Atlantic and Pacific ITCZ change. *Past Global Changes Magazine*, *25*(1) *CLIVAR Exchanges* (72). https://doi.org/10.22498/pages.25.1.52

Linsley, B. K., Rosenthal, Y., & Oppo, D. W. (2010). Holocene evolution of the Indonesian throughflow and the western Pacific warm pool. *Nature Geoscience*, *3*(8), 578–583. https://doi.org/10.1038/NGEO920

Locarnini, R. A., Mishonov, A. V., Antonov, J. I., Boyer, T. P., Garcia, H. E., Baranova, O. K., et al. (2010). In S. Levitus (Ed.), *World ocean atlas 2009, volume 1: Temperature*, *NOAA Atlas NESDIS 68* (p. 184). Washington, DC: U.S. Government Printing Office.

Lough, J. (2007). Climate and climate change on the Great Barrier Reef. In J. E. Johnson & P. A. Marshall (Eds.), *Climate change and the Great Barrier Reef: A vulnerability assessment* (pp. 15–50). Townsville: Great Barrier Reef Marine Park Authority and Australian Greenhouse Office.

Lough, J., Gupta, A. S., & Hobday, A. J. (2012). In E. S. Poloczanska, et al. (Eds.), *Temperature in a marine climate change impacts and adaptation report card for Australia 2012* (pp. 1–26). Canberra: CSIRO.

Manabe, S., & Stouffer, R. J. (1997). Coupled atmosphere-ocean model response to freshwater input: Comparison to the Younger Dryas event. *Paleoceanography*, *12*(2), 321–336. https://doi.org/10.1029/96PA03932

McCulloch, M., Mortimer, G., Esat, T., Xianhua, L., Pillans, B., & Chappell, J. (1996). High resolution windows into early Holocene climate: Sr/Ca coral records from the Huon Peninsula. *Earth and Planetary Science Letters*, *138*(1–4), 169–178. https://doi.org/10.1016/0012-821X(95)00230-A

Mix, A. C., Bard, E., & Schneider, R. (2001). Environmental processes of the ice age: Land, oceans, glaciers (EPILOG). *Quaternary Science Reviews*, *20*(4), 627–657. https://doi.org/10.1016/S0277-3791(00)00145-1

Moffa-Sanchez, P., Rosenthal, Y., Babila, T. L., Mohtadi, M., & Zhang, X. (2019). Temperature evolution of the indo-Pacific warm pool over the Holocene and the last deglaciation. *Paleoceanography and Paleoclimatology*, *34*, 1107–1123. https://doi.org/10.1029/2018PA003455

Mohtadi, M., Oppo, D. W., Steinke, S., Stuut, J.-B. W., de Pol-Holz, R., Hebbeln, D., & Lückge, A. (2014). Glacial to Holocene swings of the Australian-Indonesian monsoon. *Nature*, *509*(7498), 76–80. https://doi.org/10.1038/nature13196

Montaggioni, L. F. (2005). History of indo-Pacific coral reef systems since the last glaciation: Development patterns and controlling factors. *Earth-Science Reviews*, *71*(1–2), 1–75. https://doi.org/10.1016/j.earscirev.2005.01.002

Moreno, P. I., Denton, G. H., Moreno, H., Lowell, T. V., Putnam, A. E., & Kaplan, M. R. (2015). Radiocarbon chronology of the Last Glacial Maximum and its termination in northwestern Patagonia. *Quaternary Science Reviews*, *122*, 233–249. https://doi.org/10.1016/j.quascirev.2015.05.027

Moss, R. H., Edmonds, J. A., Hibbard, K. A., Manning, M. R., Rose, S. K., van Vuuren, D. P., et al. (2010). The next generation of scenarios for climate change research and assessment. *Nature*, *463*(7282), 747–756. https://doi.org/10.1038/nature08823

Page, M. C., & Dickens, G. R. (2005). Sediment fluxes to Marion Plateau (southern Great Barrier Reef province) over the last 130 ky: New constraints of 'transgressive shedding' off northeastern Australia. *Marine Geology*, *219*(1), 27–45. https://doi.org/10.1016/j.margeo.2005.05.002

Palumbi, S. R. (1997). Molecular biogeography of the Pacific. *Coral Reefs*, *16*(0), S47–S52. https://doi.org/10.1007/s003380050241

Patterson, M. A., Webster, J. M., Hutchings, P., Braga, J.-C., Humblet, M., & Yokoyama, Y. (2020). Bioerosion traces in the Great Barrier Reef over the past 10 to 30 kyr. *Palaeogeography, Palaeoclimatology, Palaeoecology*, *542*, 109503. https://doi.org/10.1016/j.palaeo.2019.109503

Perry, C. T., Smithers, S. G., Gulliver, P., & Browne, N. K. (2012). Evidence of very rapid reef accretion and reef growth under high turbidity and terrigenous sedimentation. *Geology*, *40*(8), 719–722. https://doi.org/10.1130/G33261.1

Pirazzoli, P. A., Radtke, U., Hantoro, W. S., Jouannic, C., Hoang, C. T., Causse, C., & Borel Best, M. (1991). Quaternary raised coral-reef terraces on Sumba Island, Indonesia. *Science*, *252*(5014), 1834–1836. https://doi.org/10.1126/science.252.5014.1834

Putnam, A. E., Schaefer, J. M., Barrell, D. J. A., Vandergoes, M., Denton, G. H., Kaplan, M. R., et al. (2010). In situ cosmogenic ^{10}Be production-rate calibration from the Southern Alps, New Zealand. *Quaternary Geochronology*, *5*(4), 392–409. https://doi.org/10.1016/j.quageo.2009.12.001

Putnam, A. E., Schaefer, J. M., Denton, G. H., Barrell, D. J., Andersen, B. G., Koffman, T. N., et al. (2013). Warming and glacier recession in the Rakaia valley, Southern Alps of New Zealand, during Heinrich Stadial 1. *Earth and Planetary Science Letters*, *382*, 98–110. https://doi.org/10.1016/j.epsl.2013.09.005

Putnam, A. E., Schaefer, J. M., Denton, G. H., Barrell, D. J. A., Birkel, S. D., Andersen, B. G., et al. (2013). The Last Glacial Maximum at 44°S documented by a ^{10}Be moraine chronology at Lake Ohau, southern Alps of New Zealand. *Quaternary Science Reviews*, *62*, 114–141.

Rasmussen, S. O., Andersen, K. K., Svensson, A. M., Steffensen, J. P., Vinther, B. M., Clausen, H. B., et al. (2006). A new Greenland ice core chronology for the last glacial termination. *Journal of Geophysical Research*, *111*, D06102. https://doi.org/10.1029/2005JD006079

Reeves, J. M., Barrows, T. T., Cohen, T. J., Kiem, A. S., Bostock, H. C., Fitzsimmons, K. E., et al. (2013). Climate variability over the last 35,000 years recorded in marine and terrestrial archives in the Australian region: An OZ-INTIMATE compilation. *Quaternary Science Reviews*, *74*, 21–34. https://doi.org/10.1016/j.quatscirev.2013.01.001

Reeves, J. M., Bostock, H. C., Ayliffe, L. K., Barrows, T. T., de Deckker, P., Devriendt, L. S., et al. (2013). Palaeoenvironmnetal change in tropical Australasia over the last 30,000 years—A synthesis by the OZ-INTIMATE group. *Quaternary Science Reviews*, *74*, 97–114. https://doi.org/10.1016/j.quatscirev.2012.11.027

Reisinger, A., Kitching, R. L., Chiew, F., Hughes, L., Newton, P. C. D., Schuster, S. S., et al. (2014). Australasia. In V. R. Barros, et al. (Eds.), *Climate change 2014: Impacts, adaptation, and vulnerability. Part B: Regional aspects. Contribution of Working Group II to the Fifth Assessment Report of the Intergovernmental Panel on Climate Change* (Chap. 25, pp. 1371–1438). Cambridge, UK and New York, NY, USA: Cambridge University Press.

Renssen, H., Mairesse, A., Goosse, H., Mathiot, P., Heiri, O., Roche, D. M., et al. (2015). Multiple causes of the Younger Dryas cold period. *Nature Geoscience*, *8*(12), 946–949. https://doi.org/10.1038/ngeo2557

Rhein, M., Rintoul, S. R., Aoki, S., Campos, E., Chambers, D., Feely, R., et al. (2013). Chapter 3, observations: Ocean. In T. F. Stocker, et al. (Eds.), *Climate change 2013: The physical science basis. Contribution of Working Group I to the Fifth Assessment Report of the Intergovernmental Panel on Climate Change* (pp. 255–315). UK: Cambridge University Press.

Rosenthal, Y., Oppo, D. W., & Linsley, B. K. (2003). The amplitude and phasing of climate change during the last deglaciation in the Sulu Sea, western equatorial Pacific. *Geophysical Research Letters*, *30*(8), 1428. https://doi.org/10.1029/2002GL016612

Sadler, J., Webb, G. E., Leonard, N. D., Nothdruft, L. D., & Clark, T. C. (2016). Reef core insights into mid-Holocene water temperatures of the southern Great Barrier Reef. *Paleoceanography*, *31*, 1395–1408. https://doi.org/10.1002/2016PA002943

Schröder, J. F., Holbourn, A., Kuhnt, W., & Küssner, K. (2016). Variations in sea surface hydrology in the southern Makassar Strait over the past 26 kyr. *Quaternary Science Reviews*, *154*, 143–156. https://doi.org/10.1016/j.quatscirev.2016.10.018

Schröder, J. F., Kuhnt, W., Holbourn, A., Beil, S., Zhang, P., Hendrizan, M., & Xu, J. (2018). Deglacial warming and hydroclimate variability in the central Indonesian archipelago. *Paleoceanography and Paleoclimatology*, *33*, 974–993. https://doi.org/10.1029/2018PA003323

Shakun, J. D., & Carlson, A. E. (2010). A global perspective on last glacial maximum to Holocene climate change. *Quaternary Science Reviews*, *29*(15–16), 1801–1816. https://doi.org/10.1016/j.quatscirev.2010.03.016

Shulmeister, J., Thackray, G. D., Rittenour, T. M., Fink, D., & Patton, N. R. (2019). The timing and nature of the last glacial cycle in New Zealand. *Quaternary Science Reviews*, *206*, 1–20. https://doi.org/10.1016/j.quatscirev.2018.12.020

Smith, R. J. (2009). Use and misuse of the reduced major axis for line-fitting. *American Journal of Physical Anthropology*, *140*(3), 476–486. https://doi.org/10.1002/ajpa.21090

Steinke, S., Glatz, C., Mohtadi, M., Groeneveld, J., Li, Q., & Jian, Z. (2011). Past dynamics of the East Asian monsoon: No inverse behaviour between the summer and winter monsoon during the Holocene. *Global and Planetary Change*, *78*(3–4), 170–177. https://doi.org/10.1016/j.gloplacha.2011.06.006

Steinke, S., Kienast, M., Groeneveld, J., Lin, L. -C., Chen, M. -T., & Rendle-Bühring, R. (2008). Proxy dependence of the temporal pattern of deglacial warming in the tropical South China Sea: Toward resolving seasonality. *Quaternary Science Reviews*, *27*(7–8), 688–700. https://doi.org/10.1016/j.quatscirev.2007.12.003

Stoll, H. M., Schrag, D. P., & Clemens, S. C. (1999). Are seawater Sr/Ca variations preserved in Quaternary foraminifer? *Geochimica et Cosmochimica Acta*, *63*(21), 3535–3547. https://doi.org/10.1016/S0016-7037(99)00129-5

Stott, L., Cannariato, K., Thunell, R., Haug, G. H., Koutavas, A., & Lund, S. (2004). Decline of surface temperature and salinity in the western tropical Pacific Ocean in the Holocene epoch. *Nature*, *431*(7004), 56–59. https://doi.org/10.1038/nature02903

Strand, P. D., Schaefer, J. M., Putnam, A. E., Denton, D. H., Barrell, D. J. A., Koffman, T. N. B., & Schwartz, R. (2019). Millennial-scale pulsebeat of glaciation in the Southern Alps of New Zealand. *Quaternary Science Reviews*, *220*, 165–177. https://doi.org/10.1016/j.quatscirev.2019.07.022

Szilagyi, Z., Webster, J. M., Patterson, M. A., Hips, K., Riding, R., Foley, M., et al. (2020). Controls on the spatio-temporal distribution of microbialite crusts on the great barrier reef over the past 30,000 years. *Marine Geology*, *429*, 106312. https://doi.org/10.1016/j.margeo.2020.106312

Tibby, J. (2012). The Younger Dryas: Relevant in the Australian region? *Quaternary International*, *253*, 47–54. https://doi.org/10.1016/j.quaint.2012.01.003

Timmerman, A., Okumura, Y., An, S.-I., Clement, A., Dong, B., Guilyardi, E., et al. (2007). The influence of a weakening of the Atlantic Meridional Overturning Circulation on ENSO. *Journal of Climate*, *20*(19), 4899–4919. https://doi.org/10.1175/JCLI4283.1

Torda, G., Donelson, J. M., Aranda, M., Barshis, D. J., Bay, L., Berumen, M. L., et al. (2017). Rapid adaptive responses to climate change in corals. *Nature Climate Change*, *7*(9), 627–636. https://doi.org/10.1038/NCLIMATE3374

van Hooidonk, R., Maynard, J. A., & Planes, S. (2013). Temporary refugia for coral reefs in a warming world. *Nature Climate Change*, *3*(5), 508–511. https://doi.org/10.1038/nclimate1829

Vandergoes, M. J., Newnham, R. M., Preusser, F., Hendy, C. H., Lowell, T. V., Fitzsimons, S. J., et al. (2005). Regional insolation forcing of late Quaternary climate change in the Southern Hemisphere. *Nature*, *436*(7048), 242–245. https://doi.org/10.1038/nature03826

Veron, J. E. N., & Done, T. J. (1979). Corals and coral communities of Lord Howe Island. *Australian Journal of Marine and Freshwater Research*, *30*(2), 203–236. https://doi.org/10.1071/MF9790203

Vincent, E. M., Lengaigne, M., Menkes, C. E., Jourdain, N. C., Marchesiello, P., & Madec, G. (2009). Interannual variability of the South Pacific Convergence Zone and implications for tropical cyclone genesis. *Climate Dynamics*, *36*(9–10), 1881–1896. https://doi.org/10.1007/s00382-009-0716-3

Waelbroeck, C., Labeyrie, L., Michel, E., Duplessy, J. C., McManus, J. F., Lambeck, K., et al. (2002). Sea-level and deep water temperature changes derived from benthic foraminifera isotopic records. *Quaternary Science Reviews*, *21*(1–3), 295–305. https://doi.org/10.1016/S0277-3791(01)00101-9

Webster, J. M., Braga, J. C., Humblet, M., Potts, D. C., Iryu, Y., Yokoyama, Y., et al. (2018). Response of the Great Barrier Reef to sea-level and environmental changes over the past 30,000 years. *Nature Geoscience*, *11*(6), 426–432. https://doi.org/10.1038/s41561-018-0127-3

Webster, J. M., Yokoyama, Y., Cotterill, C., & The Expedition 325 Scientists (2011). *Proceedings of the Integrated Ocean Drilling Program Vol. 325 (Integrated Ocean Drilling Program Management International Inc.)*. Integrated Ocean Drilling Program.

Williams, P. W., King, D. N. T., Zhao, J. X., & Collerson, K. D. (2004). Speleothem master chronologies: Combined Holocene ^{18}O and ^{13}C records form the North Island of New Zealand and their paleoenvironmental interpretation. *Holocene*, *14*(2), 194–208. https://doi.org/10.1191/0959683604hl676rp

Xu, J., Holbourn, A., Kuhnt, W., Jian, Z., & Kawamura, H. (2008). Changes in the thermocline structure of the Indonesian outflow during terminations I and II. *Earth and Planetary Science Letters*, *273*(1–2), 152–162. https://doi.org/10.1016/j.epsl.2008.06.029

Yokoyama, Y., Esat, T. M., Thompson, W. G., Thomas, A. L., Webster, J. M., Miyairi, Y., et al. (2018). Rapid glaciation and a two-step sea level plunge into the Last Glacial Maximum. *Nature*, *559*, 603–607. https://doi.org/10.1038/s41586-018-0335-4